

Shahzad G. Raja
Editor

Cardiac Surgery

A Complete Guide

EXTRAS ONLINE

 Springer

Cardiac Surgery

Shahzad G. Raja
Editor

Cardiac Surgery

A Complete Guide

 Springer

Editor

Shahzad G. Raja
Harefield Hospital
Royal Brompton & Harefield NHS Trust
London
UK

ISBN 978-3-030-24173-5 ISBN 978-3-030-24174-2 (eBook)

<https://doi.org/10.1007/978-3-030-24174-2>

© Springer Nature Switzerland AG 2020

This work is subject to copyright. All rights are reserved by the Publisher, whether the whole or part of the material is concerned, specifically the rights of translation, reprinting, reuse of illustrations, recitation, broadcasting, reproduction on microfilms or in any other physical way, and transmission or information storage and retrieval, electronic adaptation, computer software, or by similar or dissimilar methodology now known or hereafter developed.

The use of general descriptive names, registered names, trademarks, service marks, etc. in this publication does not imply, even in the absence of a specific statement, that such names are exempt from the relevant protective laws and regulations and therefore free for general use.

The publisher, the authors, and the editors are safe to assume that the advice and information in this book are believed to be true and accurate at the date of publication. Neither the publisher nor the authors or the editors give a warranty, expressed or implied, with respect to the material contained herein or for any errors or omissions that may have been made. The publisher remains neutral with regard to jurisdictional claims in published maps and institutional affiliations.

This Springer imprint is published by the registered company Springer Nature Switzerland AG
The registered company address is: Gewerbestrasse 11, 6330 Cham, Switzerland

Dedicated to my parents for their love, endless support, encouragement and sacrifices.

Preface

Cardiac Surgery: A Complete Guide provides a succinct and solid overview of the specialty of cardiac surgery. The book predominantly aimed at trainees as well as practicing surgeons presents in a clear and accessible way the most up-to-date knowledge of the entire specialty of cardiac surgery. With an emphasis on key concepts, high-yield information, and international best practice, it concisely covers the breadth of material needed for certification and practice of cardiac surgery. Thanks to the reader-friendly design, featuring an abundance of illustrations, intraoperative photographs, tables as well as information boxes, the book enables the readers to visually grasp and retain difficult concepts. Evidence-based approaches to the management of a range of cardiac surgical conditions will help readers overcome tough clinical challenges and improve patient outcomes.

Cardiac Surgery: A Complete Guide brings together experts from around the world to discuss the full scope of cardiac surgery. It provides essential, up-to-date, need-to-know information about the latest surgical perspectives and approaches to treatment including innovations in minimally invasive surgery and percutaneous devices. Drawing together current knowledge and evidence and examining all aspects of cardiac surgery in one succinct volume, *Cardiac Surgery: A Complete Guide* is the ideal resource for the trainees as well as practicing surgeons enabling them to effectively apply the latest techniques and evidence-based approaches in their day-to-day practice.

A key feature of the book is the section on Review Questions that contains Single Best Answer Questions that will prove to be an invaluable resource for residents preparing for their certification examinations. The breadth of topics covered and detailed answers expand the versatility of this book to a larger audience including doctors preparing for postgraduate exams and other allied healthcare professionals who will be examined in cardiac surgery.

The questions are in line with the most recent developments in clinical guidelines and have been written in accordance with the recent changes in certification examinations. They are designed to provide a comprehensive coverage of the cardiac surgery curriculum and are similar to those that have or will feature in certification examinations. The answers provide detailed explanations as to how the correct answer is reached, followed by a clear discussion of how the incorrect answers are ruled out and supplementary information about other important aspects of each question. The answers are designed to allow the reader to further enhance their clinical knowledge, understanding, and single best answer technique, thus making this book an excellent aid for exam preparation.

I would like to thank all the contributors who have produced excellent chapters and made this collaborative venture worthwhile. Last but not least, my special thanks to the Springer Nature team—Grant Weston, Leo Johnson, Rajeswari Balachandran, and Swathi Chandrasekar—for managing the project with courtesy and patience.

London, UK
2020

Shahzad G. Raja

Contents

Part I Perioperative Care and Cardiopulmonary Bypass

1 Cardiac Catheterization	3
Konstantinos Kalogeras and Vasileios F. Panoulas	
2 Fractional Flow Reserve	15
Vasileios F. Panoulas	
3 Echocardiography	23
Shelley Rahman Haley	
4 Cardiac Computed Tomography and Magnetic Resonance Imaging	41
Tarun K. Mittal	
5 Assessment of Myocardial Viability	55
Chandra Katikireddy, Nareg Minaskeian, Amir Najafi, and Arang Samim	
6 Blood Conservation Strategies in Cardiac Surgery	63
David Royston	
7 Inotropes, Vasopressors and Vasodilators	69
Nandor Marczin, Paola Carmona, Steffen Rex, and Eric E. C. de Waal	
8 Cardiac Pacing in Adults	81
Daniel Keene, S. M. Afzal Sohaib, and Tom Wong	
9 Adult Cardiopulmonary Bypass	93
Demetrios Stefanou and Ioannis Dimarakis	
10 Myocardial Protection in Adults	101
Francesco Nicolini and Tiziano Gherli	
11 Heparin-Induced Thrombocytopenia	109
Benilde Cosmi	
12 Tissue Sealants in Cardiac Surgery	119
Louis P. Perrault and Fatima Zohra Moukhariq	

Part II Coronary Artery Disease

13 Conduits for Coronary Artery Bypass Surgery	131
Cristiano Spadaccio and Mario F. L. Gaudino	
14 Endoscopic Saphenous Vein and Radial Artery Harvesting	139
Fabrizio Rosati and Gianluigi Bisleri	
15 Conventional Coronary Artery Bypass Grafting	149
Kirthi Ravichandren and Faisal G. Bakaeen	

16	Off-Pump Coronary Artery Bypass Grafting	157
	Shahzad G. Raja and Umberto Benedetto	
17	Minimally Invasive Coronary Artery Bypass Grafting	167
	Ming Hao Guo, Janet M. C. Ngu, and Marc Ruel	
18	Totally Endoscopic Coronary Artery Bypass Grafting	175
	Brody Wehman and Eric J. Lehr	
19	Redo Coronary Artery Bypass Grafting	185
	Hitoshi Yaku, Sachiko Yamazaki, and Satoshi Numata	
20	Hybrid Coronary Revascularization	193
	Elbert E. Williams, Gianluca Torregrossa, and John D. Puskas	
21	Bilateral Internal Mammary Artery Grafting	199
	Shahzad G. Raja and David Taggart	
22	Total and Multiple Arterial Revascularization	207
	James Tatoulis	
23	Anastomotic Devices for Coronary Artery Surgery	219
	Nirav C. Patel and Jonathan M. Hemli	
24	Post-infarction Ventricular Septal Defect	229
	Joseph Nader, Pierre Voisine, and Mario Sénéchal	
25	Ischemic Mitral Regurgitation	237
	Michael Salna and Jack H. Boyd	
26	Post-infarction Ventricular Aneurysms	243
	Manish K. Soni and Shahzad G. Raja	
27	Coronary Endarterectomy	253
	Nikolaos A. Papakonstantinou	
28	Transmyocardial Laser Revascularization	261
	Justin G. Miller and Keith A. Horvath	
29	Gene Therapy for Coronary Artery Disease	269
	Vivekkumar B. Patel, Christopher T. Ryan, Ronald G. Crystal, and Todd K. Rosengart	
30	Combined Carotid and Coronary Artery Disease	277
	Salah E. Altarabsheh, Carolyn Chang, Yakov E. Elgudin, and Salil V. Deo	
31	Coronary Artery Aneurysms and Fistulas	281
	Aimee Wehber, Kevin Oguayo, Joseph Pendley, Jonathan J. Allred, J. Christopher Scott, and William Jeremy Mahlow	
Part III Valvular Heart Disease		
32	Mechanical Prosthetic Valves	291
	Matthew C. Henn and Marc R. Moon	
33	Stented Bioprosthetic Valves	299
	Giuseppe Santarpino and Shahzad G. Raja	
34	Bentall and Mini-Bentall Procedure	307
	Adam Chakos and Tristan D. Yan	

35	Aortic Valve-Sparing Root Replacement	315
	Mateo Marin-Cuartas and Michael A. Borger	
36	Aortic Valve Repair	325
	Igo B. Ribeiro and Munir Boodhwani	
37	The Small Aortic Root	345
	John R. Doty	
38	The Ross Procedure	351
	Ismail Bouhout and Ismail El-Hamamsy	
39	Bicuspid Aortic Valve and Aortopathy	359
	Sri Harsha Patlolla and Hartzell V. Schaff	
40	Mitral Valve Replacement	373
	David Blitzer, Jeremy J. Song, and Damien J. LaPar	
41	Techniques for Mitral Valve Repair	381
	Bassman Tappuni, Hoda Javadikasgari, Bajwa Gurjyot, and Rakesh M. Suri	
42	Mitral Valve Repair in Rheumatic Mitral Disease	389
	Taweesak Chotivatanapong	
43	Native Valve Endocarditis	397
	Kareem Bedeir and Basel Ramlawi	
44	Prosthetic Valve Endocarditis	405
	Bobby Yanagawa, Maral Ouzounian, and David A. Latter	
45	Tricuspid Valve Surgery	415
	Christoph T. Starck and Volkmar Falk	
46	Minimally Invasive Aortic Valve Surgery	421
	Mattia Glauber and Antonio Miceli	
47	Minimally Invasive Mitral Valve Surgery	429
	Mateo Marin-Cuartas and Piroze M. Davierwala	
48	Transcatheter Aortic Valve Therapies	437
	Mohanad Hamandi and Michael J. Mack	
49	Transcatheter Pulmonary Valve Replacement	447
	Hussam S. Suradi and Ziyad M. Hijazi	
50	Transcatheter Mitral Valve Therapies	455
	Adolfo Ferrero Guadagnoli, Maurizio Taramasso, and Francesco Maisano	
51	Carcinoid Heart Disease	463
	Anita Nguyen, Hartzell V. Schaff, and Heidi M. Connolly	

Part IV Thoracic Aorta

52	Acute Type A Aortic Dissection	475
	Alice Le Huu, Umang M. Parikh, and Joseph S. Coselli	
53	Acute Type B Aortic Dissection	487
	Ashraf A. Sabe and G. Chad Hughes	
54	Chronic Type B Aortic Dissection	497
	Konstantinos Spanos and Tilo Kölbel	

55	Aortic Intramural Hematoma and Penetrating Aortic Ulcer	507
	Abe DeAnda Jr. and Christine Shokrzadeh	
56	Descending Thoracic and Thoracoabdominal Aortic Aneurysms	515
	Konstadinos A. Plestis, Oleg I. Orlov, Vishal N. Shah, Robert J. Meisner, Cinthia P. Orlov, and Serge Sicouri	
57	Aortic Arch Aneurysms	529
	Mahnoor Imran, Mohammad A. Zafar, Tamta Chkhikvadze, Bulat A. Ziganshin, and John A. Elefteriades	
58	Hybrid Aortic Arch Repair	545
	Oliver J. Liakopoulos, Julia Merkle, and Thorsten Claus W. Wahlers	
59	Endovascular Stent Grafting of Thoracic Aorta	553
	David Tobey, Allan Capote, Rodney White, and Ali Khoynezhad	
60	Neuroprotective Strategies During Aortic Surgery	561
	Jee Young Kim, Helen A. Lindsay, and George Djaiani	
61	Sinus of Valsalva Aneurysms	567
	Manish K. Soni and Shahzad G. Raja	
62	Elephant Trunk Procedures	573
	Suyog A. Mokashi and Lars G. Svensson	
63	Porcelain Ascending Aorta	579
	Yigal Abramowitz and Raj R. Makkar	
64	Cardiovascular Manifestations of Marfan and Loeys-Dietz Syndrome	587
	Florian S. Schoenhoff and Thierry P. Carrel	
 Part V Mechanical Circulatory Support and Transplantation		
65	Pharmacologic Support of the Failing Heart	597
	Haifa Lyster and Georgios Karagiannis	
66	Cardiac Resynchronization Therapy for Heart Failure	607
	Mumin R. Noor, Rebecca E. Lane, and Owais Dar	
67	Intra-aortic Balloon Pump	613
	Nnamdi Nwaejike and Mani A. Daneshmand	
68	Extracorporeal Life Support in the Adult	623
	Adeel Abbasi and Corey E. Ventetuolo	
69	Temporary Circulatory Support Devices	631
	Gerin R. Stevens and Brian Lima	
70	Heart Transplantation	639
	Aravinda Page and Yasir Abu-Omar	
71	Heart-Lung Transplantation	645
	Don Hayes Jr., Michael S. Mulvihill, and David McGiffin	
72	Immunosuppression in Cardiac Transplantation	655
	Yu Xie, Kevin W. Lor, and Jon A. Kobashigawa	
73	Complications of Heart Transplantation	665
	Mayooran Shanmuganathan and Owais Dar	

Part VI Miscellaneous Cardiovascular Disorders

- 74 Cardiac Tumors** 673
 Maria Romero and Renu Virmani
- 75 Concomitant Coronary Artery Disease and Lung Cancer** 691
 Wilhelm P. Mistiaen
- 76 Trauma to the Heart and Great Vessels** 697
 Ankur Bakshi, Matthew J. Wall Jr., and Ravi K. Ghanta
- 77 Pericardial Diseases** 703
 Rolando Calderon-Rojas and Hartzell V. Schaff
- 78 Pulmonary Thromboendarterectomy** 717
 Michael M. Madani and Jill R. Higgins
- 79 Surgical Management of Atrial Fibrillation** 727
 Kareem Bedeir and Basel Ramlawi
- 80 Hypertrophic Cardiomyopathy** 735
 Hao Cui and Hartzell V. Schaff
- 81 Left Ventricular Volume Reduction** 749
 Antonio M. Calafiore, Massimiliano Foschi, Antonio Totaro, Piero Pelini,
 and Michele Di Mauro
- 82 Renal Failure After Cardiac Surgery** 755
 Marc Vives and Juan Bustamante-Munguira
- 83 Bleeding and Re-exploration After Cardiac Surgery** 763
 Xun Zhou, Cecillia Lui, and Glenn J. R. Whitman
- 84 Sternal Wound Infections** 769
 Tomas Gudbjartsson
- 85 Atrioventricular Disruption** 777
 Sheena Garg and Shahzad G. Raja

Part VII Paediatric and Congenital Heart Disease

- 86 Pediatric Cardiopulmonary Bypass and Hypothermic Circulatory Arrest** ... 783
 Craig M. McRobb, Scott Lawson, Cory Ellis, and Brian Mejak
- 87 Myocardial Protection in Children** 791
 Abdullah Doğan and Rıza Türköz
- 88 Pediatric Extracorporeal Membrane Oxygenation and Mechanical
 Circulatory Assist Devices** 797
 Akif Ündar, Shigang Wang, Madison Force, and Morgan K. Moroi
- 89 Palliative Operations for Congenital Heart Disease** 813
 Masakazu Nakao and Roberto M. Di Donato
- 90 Coronary Anomalies in Children** 821
 Phan-Kiet Tran and Victor T. Tsang
- 91 Congenital Valvar and Supravalvar Aortic Stenosis** 829
 Viktor Hraska and Joseph R. Block

92	Atrial Septal Defects	839
	Iman Naimi and Jason F. Deen	
93	Isolated Ventricular Septal Defect	849
	Sian Chivers and Attilio A. Lotto	
94	Patent Ductus Arteriosus	865
	Robroy H. MacIver	
95	Aortopulmonary Window	869
	G. Deepak Gowda and B. C. Hamsini	
96	Coarctation of the Aorta	875
	Shafi Mussa and David R. Anderson	
97	Pulmonary Valve Stenosis	885
	Fazal W. Khan and M. Sertaç Çiçek	
98	Truncus Arteriosus	891
	Sandeep Sainathan, Ken-Michael Bayle, Christopher J. Knott-Craig, and Umar S. Boston	
99	Transposition of the Great Arteries	897
	Erik L. Frandsen and Matthew D. Files	
100	Congenitally Corrected Transposition of the Great Arteries	905
	Michel N. Ilbawi, Chawki El-Zein, and Luca Vricella	
101	Tetralogy of Fallot	917
	Damien J. LaPar and Emile A. Bacha	
102	Hypoplastic Left Heart Syndrome	923
	David J. Barron	
103	Congenital Aortic Arch Interruption and Hypoplasia	933
	Serban C. Stoica	
104	Pulmonary Atresia with Intact Septum	941
	Imran Saeed	
105	Complete Atrioventricular Septal Defect	949
	Tom R. Karl, Nelson Alphonso, John S. K. Murala, and Kanchana Singappulli	
106	Double Outlet Right Ventricle	961
	Ravi S. Samraj, Ross M. Ungerleider, and Inder Mehta	
107	Neonatal Ebstein's Anomaly	971
	Umar S. Boston, Ken Bayle, T. K. Susheel Kumar, and Christopher J. Knott-Craig	
108	Vascular Rings and Pulmonary Artery Sling	981
	Carl L. Backer	
109	Congenital Left Ventricular Outflow Tract Obstruction	993
	Imran Saeed	
110	Pediatric Heart Transplantation	1001
	James K. Kirklin	
	Review Questions	1011
	Answers	1033
	Index	1061

Part I

Perioperative Care and Cardiopulmonary Bypass

High Yield Facts

- Selective coronary angiography was first described by Mason Sones in 1958.
- The main goals of invasive coronary angiography are to confirm the presence and nature of coronary artery disease, to assess the location and extent of luminal stenosis and finally, to decide upon the optimal therapeutic approach.
- Coronary angiography is a relatively safe procedure in experienced hands with a mortality rate of 1/1000.
- Ongoing infections, acute kidney injury or failure, severe anemia, active bleeding, previous allergic reaction to contrast and severe electrolyte imbalance are considered relative contraindications.

further developed by Kurt Amplatz and Melvin Judkins in 1967 (Fig. 1.1) [2]. The coronary arteries soon became the most frequently examined vessels, using mainly pre-shaped femoral catheters by Judkins, but also those by Bourassa, Schoonmaker, King, El Gamal and many others. After the establishment of coronary angiography, a new era began in September 1977 when the first coronary angioplasty was achieved by Andreas Gruentzig [3].

Invasive Diagnostic Coronary Angiography

Coronary angiography is an integral part of the workup of patients with heart disease and a key element in the evaluation of patients with coronary artery disease (CAD). The main

History of Cardiac Catheterization

Although the first cardiac catheterization in animals was performed by the French physiologist Claude Bernard in 1840s, it was not before 1929 when the first right heart catheterization was done in human by the German doctor Werner Forssmann on himself. Selective coronary angiography was first described by Mason Sones in 1958, while special catheters for coronaries engagement and contrast injection were

K. Kalogeras
Royal Brompton and Harefield NHS Foundation Trust,
Harefield, UK

V. F. Panoulas (✉)
Royal Brompton and Harefield NHS Foundation Trust,
Harefield, UK

National Heart and Lung Institute, Imperial College London,
London, UK
e-mail: v.panoulas@imperial.ac.uk



Fig. 1.1 Melvin Paul Judkins (1922–1985) with his pre-shaped coronary catheters for femoral access (Reprinted from “The PCR-EAPCI Textbook”, chapter: A history of cardiac catheterization, Authors: Michel E. Bertrand, Bernhard Meier [1])

goals of invasive coronary angiography are to confirm the presence and nature of CAD, to assess the location and extent of luminal stenosis and finally, to decide upon the optimal therapeutic approach. Today, the simple coronary angiography has been further enriched by functional evaluation by means of intracoronary pressure measurements and anatomical evaluation using advanced intracoronary imaging modalities. Although coronary angiography is a relatively safe procedure in experienced hands (mortality rate of 1/1000), it can rarely be potentially harmful [4, 5].

Indications

A coronary angiogram is indicated as an *elective procedure*

- For any patient in whom a diagnosis of CAD is suspected or made on clinical grounds or based on additional non-invasive stress tests for the purpose of confirming the diagnosis as well as for defining the optimal therapeutic strategy.
- As part of the preoperative work-up in patients planned for a major non-cardiac or valvular cardiac surgery.

On an *emergency* basis, all patients presenting with acute ST-elevation myocardial infarction (STEMI) should undergo a coronary angiogram and a percutaneous coronary intervention (PCI) within 90 min from presentation [6].

On a *semi-urgent* basis, coronary angiography is indicated for all patients presenting with non ST elevation acute coronary syndromes (NSTEACS) including unstable angina or non-STEMI (NSTEMI) within a timeframe, defined by risk stratification scores [7].

Ongoing infections, acute kidney injury or failure, severe anemia, active bleeding, previous allergic reaction to contrast and severe electrolyte imbalance are considered relative contraindications. However, each patient should be evaluated separately and analyzed on a risk-benefit basis.

Pre-procedure Preparation

Following history and clinical examination, a written informed consent should be obtained in every patient following a clear and full description of the indication(s), the procedure and the treatment options. A routine recent set of blood samples (within a week), is required to ensure patient safety. From the hematology profile, hemoglobin, white cell and platelets count are important [8] to ensure there is no recent or occult blood loss, no underlying infection or thrombocytopenia. With regards to biochemistry tests, creatinine, urea and liver profile are equally important to ensure absence

of kidney or liver injury. Bleeding history and evidence of elevated international normalized ratio (INR) or activated partial thromboplastin time (aPTT) are elements of great importance to ensure patient safety. In patients who are anticoagulated (warfarin, novel oral anticoagulants) and managed with transradial approach, there is increased confidence to do diagnostic angiography without treatment interruption [9, 10]. However, elective percutaneous interventions, including pressure wire measurements, should not be performed in anticoagulated patients as the risk of bleeding complications rises.

A transthoracic echocardiogram [11] prior to any coronary catheterization is essential to identify regional wall motion abnormalities, valvular disease or left ventricular thrombus, information that will guide the decision making during coronary angiography.

There is evidence to support the pre-hydration before administration of contrast medium, particularly in patients at risk of contrast induced nephropathy (CIN). However, the modalities of fluid administration remain uncertain [12]. Patient's hydration status should be assessed prior to the procedure, while the aim is to have the patient euvolemic or even slightly hypervolemic before the angiogram. For most patients 1000 ml of 0.9% saline infused over 6 h is considered sufficient. Although not proven, it is considered reasonable to routinely pre-hydrate all patients regardless of renal function [13, 14].

Technical Aspects of the Procedure

Access

This can be gained through femoral, radial, ulnar, brachial or in rare circumstances, axillary/subclavian artery approach. However, transradial approach has mostly replaced the other techniques, becoming the most popular approach, due to the better hemostasis control, faster patient mobilization and increased patient comfort, while data suggest that it is associated with reduced vascular and bleeding complications alongside reduced mortality, particularly in emergency cases [15, 16]. The Seldinger technique used for access is shown in Fig. 1.2. Subsequently, all catheters can be introduced through the sheath and over a J guidewire to the aortic root, to avoid dissecting the vasculature. Problems that can be encountered in advancing the guidewire include severe arterial tortuosity, stenosis, occlusion or dissection. Such difficulties can be overcome only by understanding the anatomy using peripheral contrast injections and the appropriate use of kit (e.g., hydrophilic wires (e.g., Terumo®) or insertion of long sheaths (45 cm), use of guide rather than diagnostic catheters, use of stiff wires (Amplatz super stiff)), ensuring optimal catheter and/or wire manipulation at all times.

Fig. 1.2 Vascular access for percutaneous insertion of a sheath (a) Vessel punctured with the needle until blood back flows. (b) A flexible J-tip guidewire advanced through the needle into the vessel lumen. (c) The needle removed, and the wire is left in place. The hole around the wire can be enlarged with a scalpel. (d) Sheath and dilator placed over the guidewire. (e) Sheath and dilator advanced, over the guidewire, into the vessel. (f) Dilator and guidewire removed, while sheath is left in the vessel

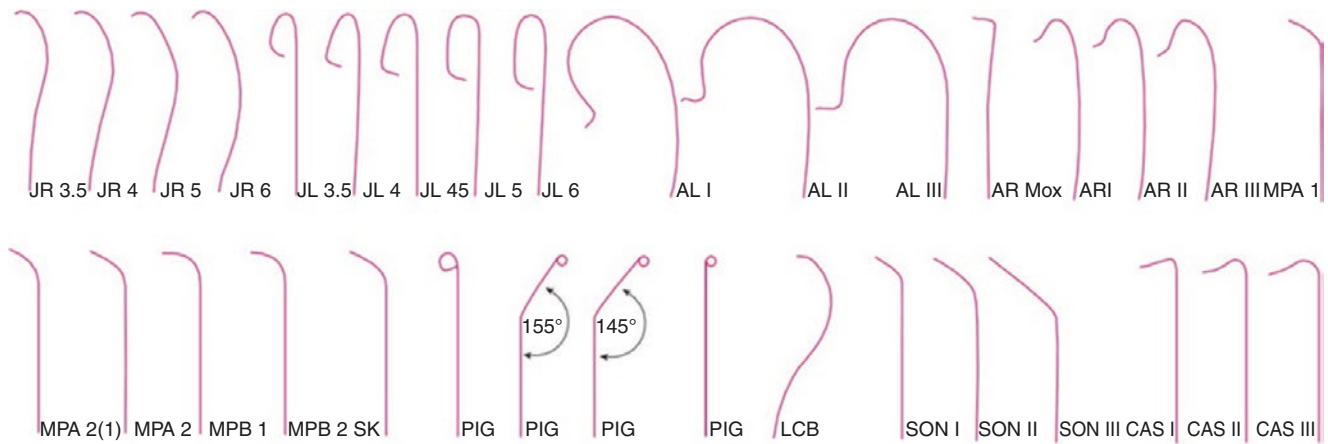
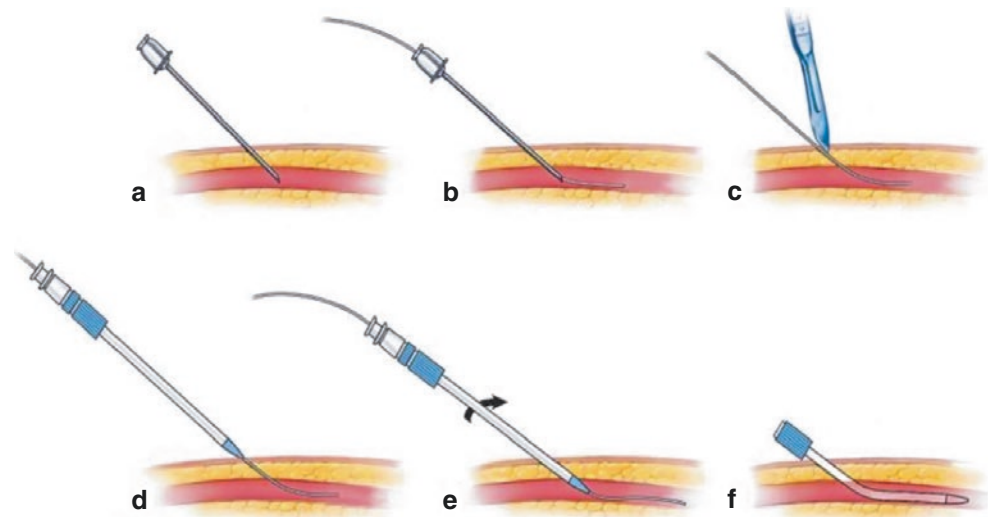


Fig. 1.3 Different catheters available for diagnostic coronary angiography (Reprinted from “The PCR-EAPCI Textbook”, chapter: Invasive diagnostic coronary angiography, Authors: Guy R. Heyndrickx, Aaron

J. Peace, Chrysafios Girasis, Christoph K. Naber, Christos V. Bourantas, Patrick W. Serruys [17])

Pharmacology

Intra-arterial administration of verapamil or nitrates via the radial sheath is used to limit the occurrence of vascular spasm, an issue not encountered with transfemoral access. Vascular spasm, as well as patient anxiety can be effectively addressed with the use of sedation prior to coronary angiogram. With regards to anticoagulation, for routine transradial diagnostic coronary angiography, an intravenous bolus of 2500–5000 units of unfractionated heparin is adequate for optimal short-term anticoagulation to avoid radial artery occlusion. Finally, it is general practice to administer nitrates (sublingual, intravenous or intracoronary) before starting the coronary angiographic injections to obtain maximal coronary dilatation and prevent potential arterial spasm at the time of catheter manipulation.

Catheter Selection and Manipulation

Improvements in catheter technology have allowed the gradual decrease of diagnostic catheters' size from 8 Fr during the early years of coronary angiography to 6 Fr and even 5 or 4 Fr size catheters. The Judkins left and right (JL/JR) pre-shaped catheters are the most commonly used catheters in the world for engaging the left and the right coronary arteries, respectively. Other pre-shaped catheters (e.g., Amplatz) can be used for injecting both coronary vessels (Fig. 1.3). While initially the same type of preformed catheters were used for the radial approach, more dedicated catheters are now available for radial procedures such as the Kimny (Boston Scientific®), Optitorque Tiger, Jacky and Sarah (Terumo®), Sones (Cordis®) and PaPa (Medtronic®) catheters which allow for engagement of both coronary ostia without need for exchanging catheters.

Angiographic Views

Angiographic views are labelled according to the position of the C-arm image receptor (the flat portion of the C-arm positioned over the patient) in relation to the patient. In the left anterior oblique (LAO) and right anterior oblique [15] the X-ray machine is positioned on the left or right side of the patient respectively, while in the cranial (CRAN) and caudal (CAUD) views the machine is positioned cranially or caudally respectively. When the receptor is in the midline then the term postero-anterior (PA) is used.

Left coronary angiography can be performed by using a wide range of catheters, depending on the approach used (radial, femoral, other) and other anatomic variables including aortic root size, coronary ostia location (high, low, anterior, posterior) and coronary artery take off (superior, horizontal, inferior, Shepherds crook). Before engaging and making injections to the left main or any vessel it is important to recognize that blood is coming freely from the catheter ensuring that the catheter has been purged of air and that a satisfactory arterial pressure trace is obtained. Any reduction in arterial pressure or change in the morphology of the arterial waveform (ventricularization—low diastolic values), should alert the operator that the catheter is obstructing flow, due to either the presence of a true ostial stenosis, or deep catheter engagement (Fig. 1.4). Although individual preferences between operators exist as to which angiographic views and in what order to be obtained, paired orthogonal views are generally required for a correct diagnosis and adequate treatment guidance (Fig. 1.5a, b). Most commonly used views include: RAO caudal, PA caudal, LAO caudal

(also termed spider), LAO cranial, PA cranial and RAO cranial.

The right coronary artery (RCA) is intubated in the LAO projection (Fig. 1.6). One of the easy ways to recognize the type of view is the presence (in all cranial vies) or absence (in all caudal views) of the diaphragm. Furthermore to identify whether the projection is LAO or RAO one has to locate the spine which should be seen at the contralateral site of the image in relation to the projection—i.e., on the right of the image in an LAO view.

In 10%–15% of cases an abnormal origin of the RCA complicates the search for the right coronary ostium. A multipurpose, a 3DRC or Williams, an Amplatz right or Amplatz left catheter can be used in these circumstances. For the RCA three views, the LAO, RAO and LAO cranial (20/20) or PA cranial (showing the bifurcation-crux to PDA and PL) are usually sufficient to identify all stenoses. On rare occasions, the left circumflex artery (LCx) can be seen originating from the right coronary sinus (Fig. 1.7).

Left ventricular angiography used to be an essential part of invasive coronary angiogram with pigtail catheters being the first choice. After entering the left ventricle cavity, a correct measurement of the left ventricular end diastolic pressure is the first and most important measurement to evaluate global LV function, while during catheter withdrawal, the pressure gradient across the aortic valve should be measured. Apart from pressure evaluation, left ventriculography offers a lot of information regarding the regional wall motion function of the left ventricle. Usually, it is obtained in two orthogonal views, RAO (30°) and LAO (40°–60°).

Fig. 1.4 Waveform of pressure ventricularization during coronary ostia engagement due to forward blood flow obstruction



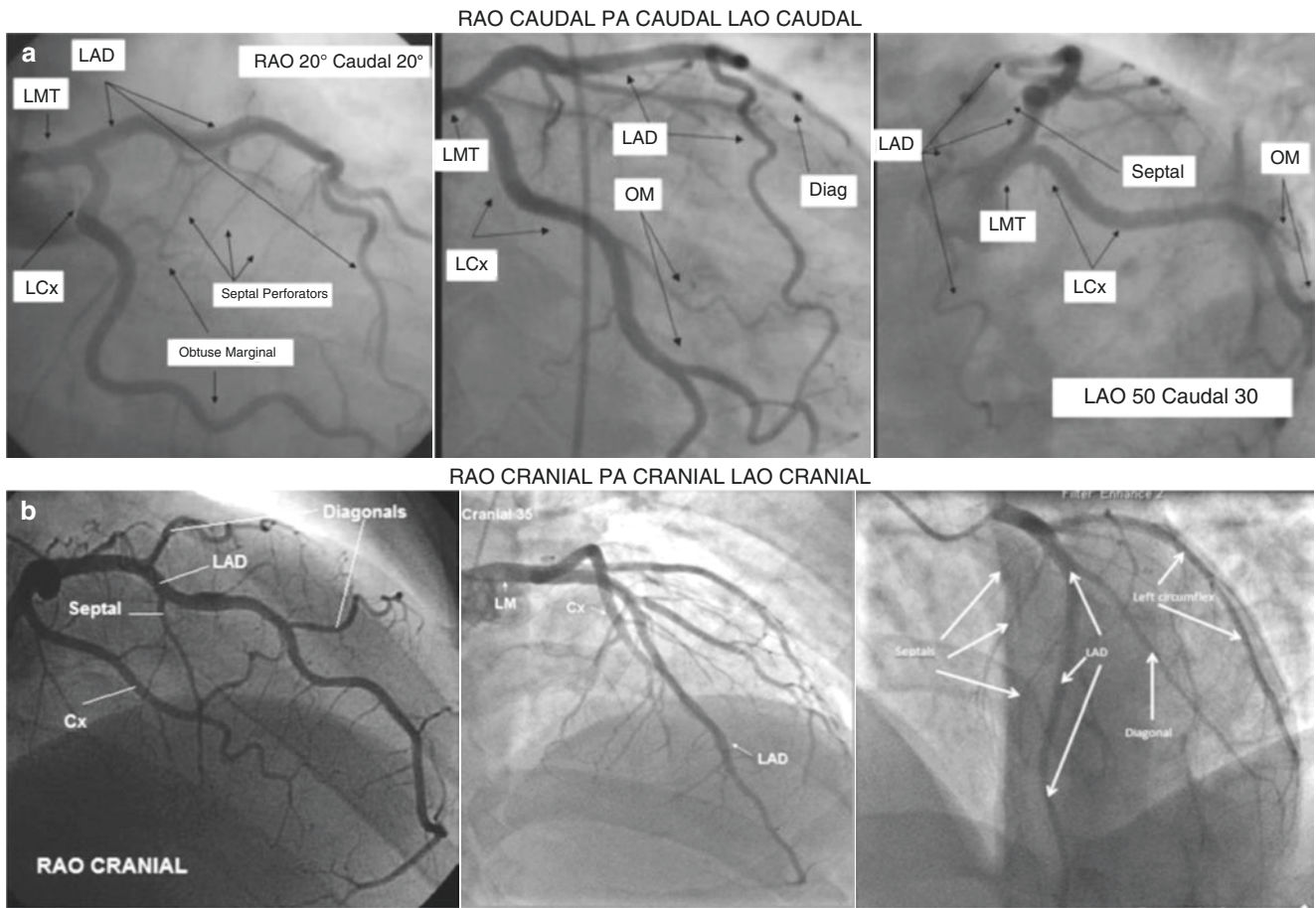


Fig. 1.5 (a) Angiographic caudal views of the left coronary artery system. (b) Angiographic cranial views of the left coronary artery system. *LMT* left main stem, *LAD* left anterior descending, *LCX* left Circumflex, *OM* oblique marginal, *Diag* diagonal

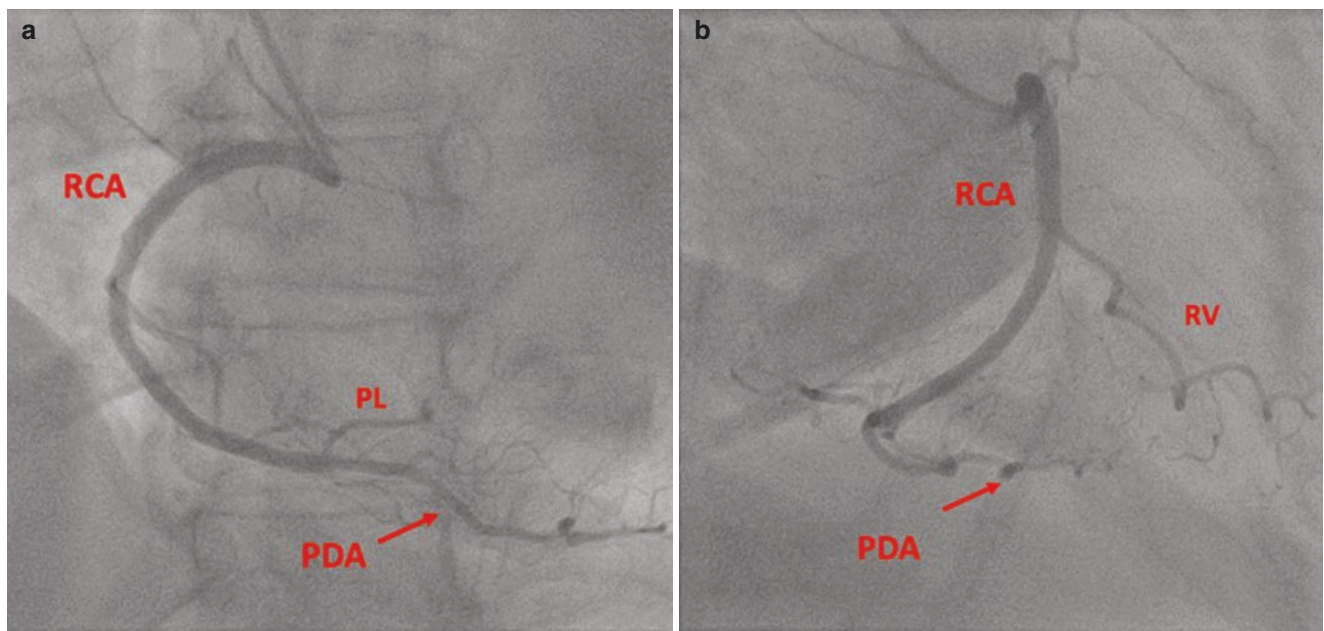


Fig. 1.6 Angiographic views of the right coronary artery (RCA). (a) Left anterior oblique view (LAO). (b) Right anterior oblique. (*RCA* right coronary artery, *PDA* posterior descending artery, *PL* posterolateral branch, *RV* right ventricle branch)

Post-procedure Care

Sheath Removal and Closure Devices

Standard manual compression after sheath removal is usually enough to acquire haemostasis after transfemoral approach diagnostic angiography. However, several vascular closure devices have been introduced to alleviate potential bleeding complications; these can be suture-based (Prostar, Proglide etc.), collagen-based (Angioseal), non-collagen based or clip closure [18, 19]. In case of transradial access, manual compression can often stop the bleeding, while a number of devices have been designed to provide haemostasis (e.g., TR band).

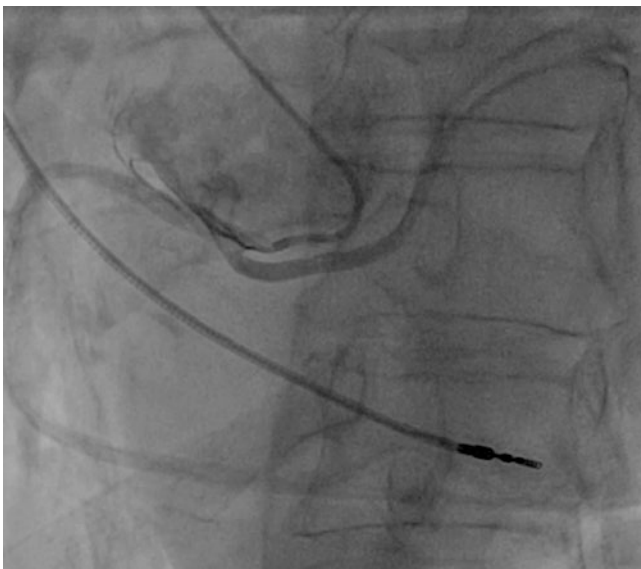


Fig. 1.7 Anomalous origin of the left circumflex artery (LCx) from the right coronary sinus

Coronary Angiogram Analysis

The conventional angiographic classification is based on visual estimation of the diameter reduction of the stenosis compared to a normal segment. The severity classification ranges from low grade stenosis (<49%), to intermediate grade (50–74%), high grade (75–90%), subtotal (91–99%) and total occlusion (100%) [20]. Further parameters required to describe in detail a coronary lesion, are the length of the stenosis, the eccentricity, tortuosity, degree of calcification, and relation to bifurcation. A number of scoring systems have been proposed to describe coronary anatomy, like the ACC/AHA Classification, the Leaman score and the SYNTAX score [21–24].

Examples of coronary lesions are shown in Figs. 1.8–1.11; Fig. 1.8 demonstrates a subtotal occlusion of the ostia of the intermediate and the left circumflex in a primary setting requiring urgent left main trifurcation stenting. In Fig. 1.9 significant mid RCA (a) and mid LCx (b) lesion are shown pre and post PCI. Figure 1.10 shows examples of LMS disease, distal (a) or diffuse/body (b). Finally, in Fig. 1.11 a tight proximal LAD lesion is shown pre- and post-PCI.

Complications

Coronary angiography is not harmless and carries a certain mortality and morbidity risk. The frequency of serious complications, such as death, myocardial infarction or cerebro-vascular accident with permanent damage, is very low (0.1–0.2%) and is usually attributed to high risk patients. Access site complications, including pseudoaneurysms or hematomas requiring blood transfusions, can occur mainly in case of transfemoral access with an incidence of 2–5%.

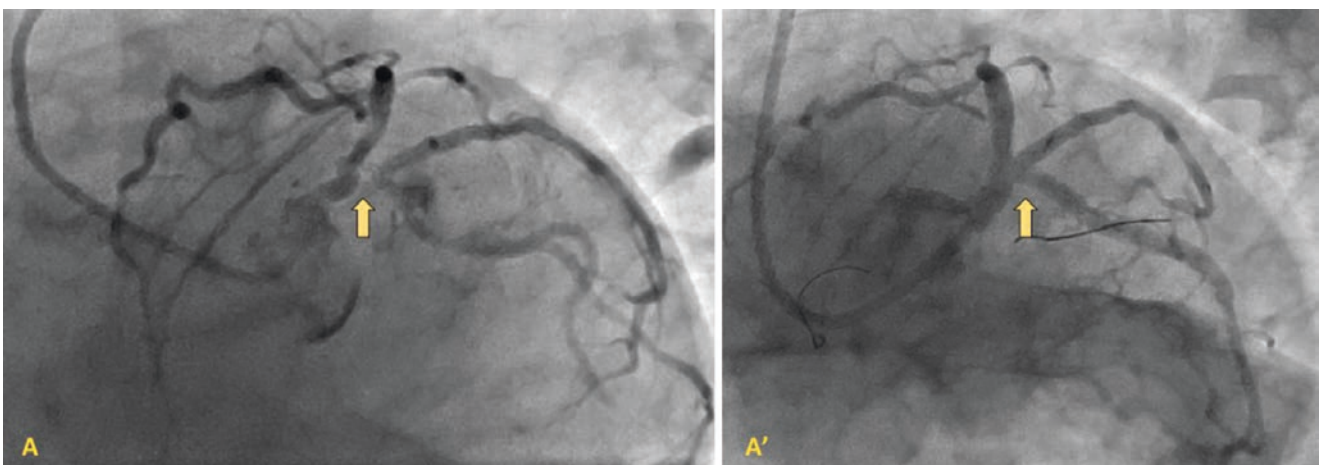


Fig. 1.8 Subtotal occlusion of ostial intermediate and LCx involving the left main stem (LMS) before (a) and after (a') primary PCI of the trifurcation

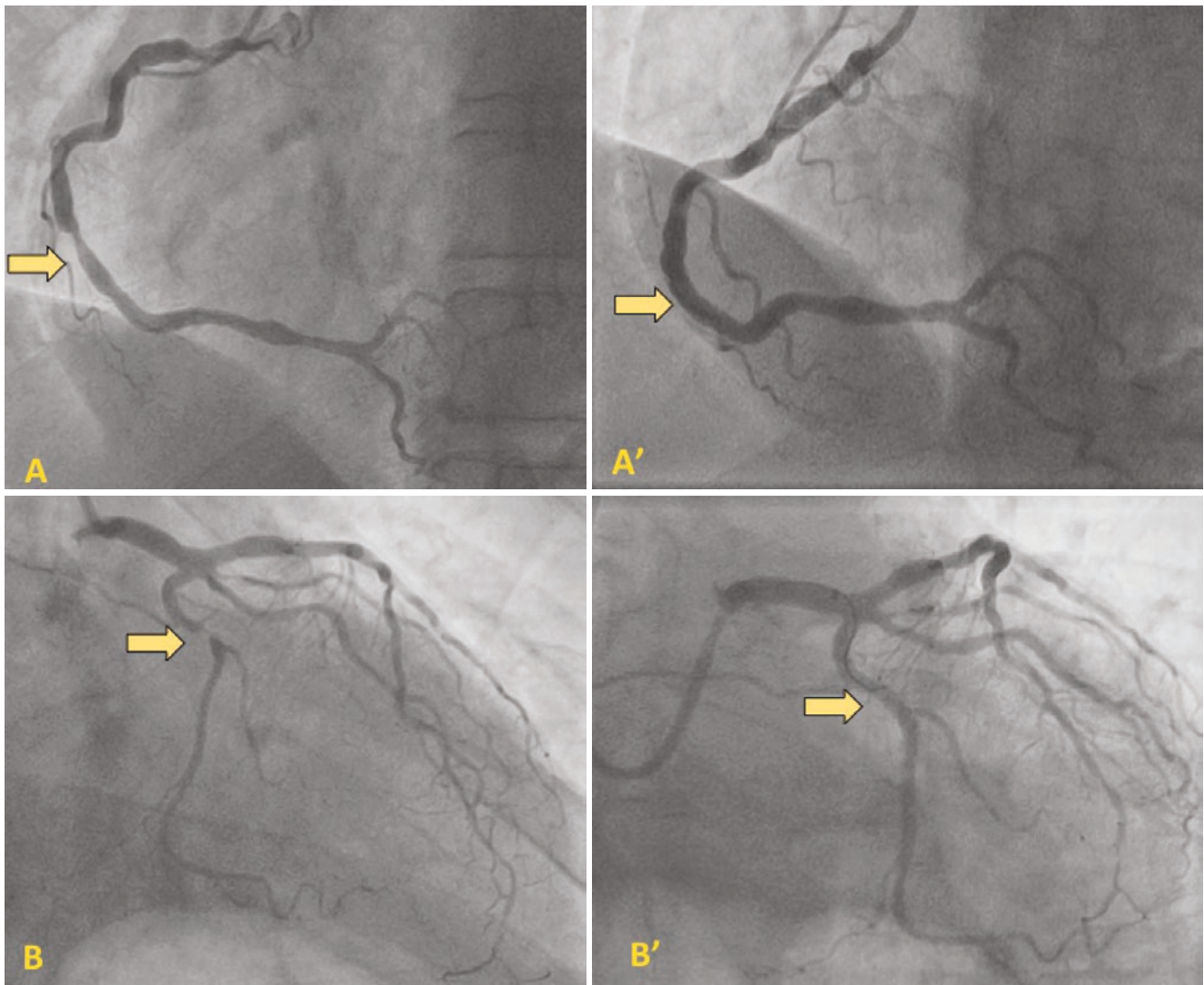


Fig. 1.9 Significant mid right coronary artery (RCA) lesion (a) treated with percutaneous coronary intervention (PCI) (a'). Tight mid LCx lesion (b) also treated with PCI (b')

With the newer generation of contrast agents, allergic reactions are becoming less frequent. However, severe reactions, including prolonged hypotension, bronchospasm, laryngeal edema, and severe anaphylactic shock have been reported. Severe hypotension during a coronary angiogram can be caused due to vasovagal reaction, drug reaction, cardiac tamponade, coronary dissection/occlusion/perforation retroperitoneal bleeding or anaphylactic shock. Furthermore, pulmonary edema can occur after contrast and volume loading especially in those patients with an already decreased left ventricular function. Transient myocardial ischemia can be caused by accidental air bubble injection. Finally, severe complications can occur by catheter manipulation or forceful against the wall injections, causing dissection of the aortic root or coronary ostia.

Right Heart Catheterization

Indications

Pulmonary artery catheters (PACs), also called Swan-Ganz catheters, are used for the management of critically ill patients, and for the evaluation of unexplained dyspnoea or suspected pulmonary hypertension. They are particularly helpful in the acute setting in the management of severe cardiogenic shock. In an elective setting, right heart catheterization (RHC) is the cornerstone for the diagnosis and follow up of pulmonary artery hypertension. Furthermore, RHC can be helpful in identifying the severity of other underlying cardio-pulmonary diseases (e.g., congenital heart disease, left-to-

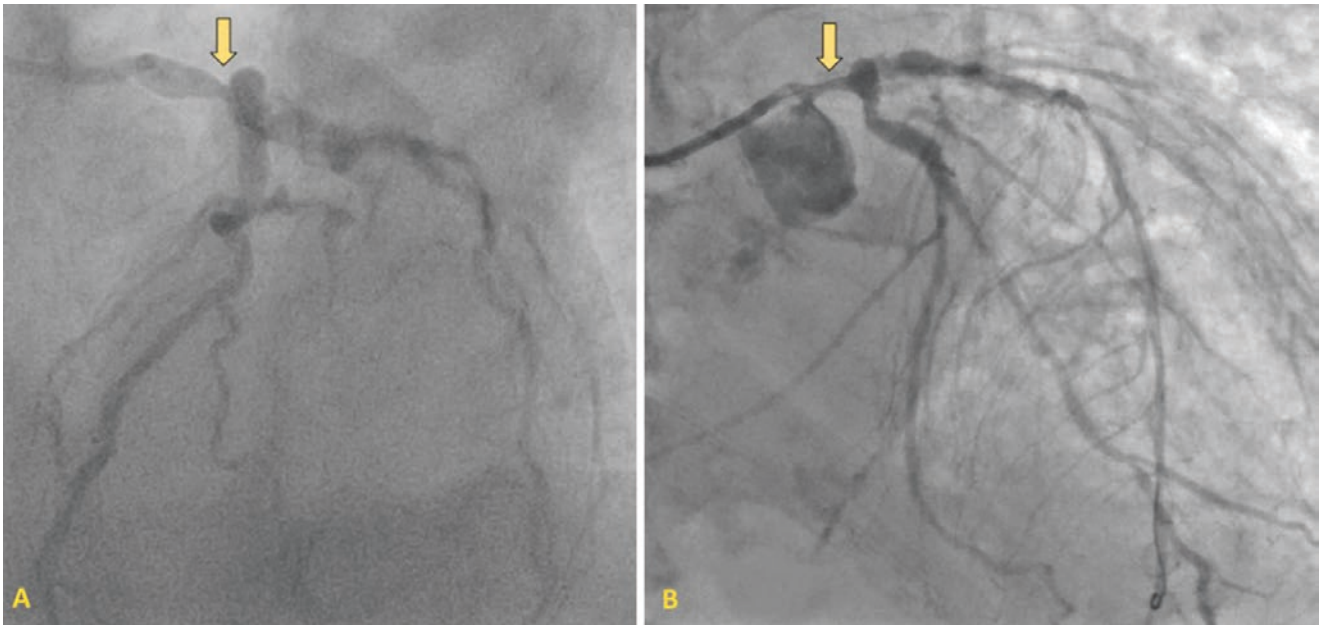


Fig. 1.10 Different patterns of left main stem (LMS) disease. Distal LMS (a) versus diffuse calcific body disease (b)

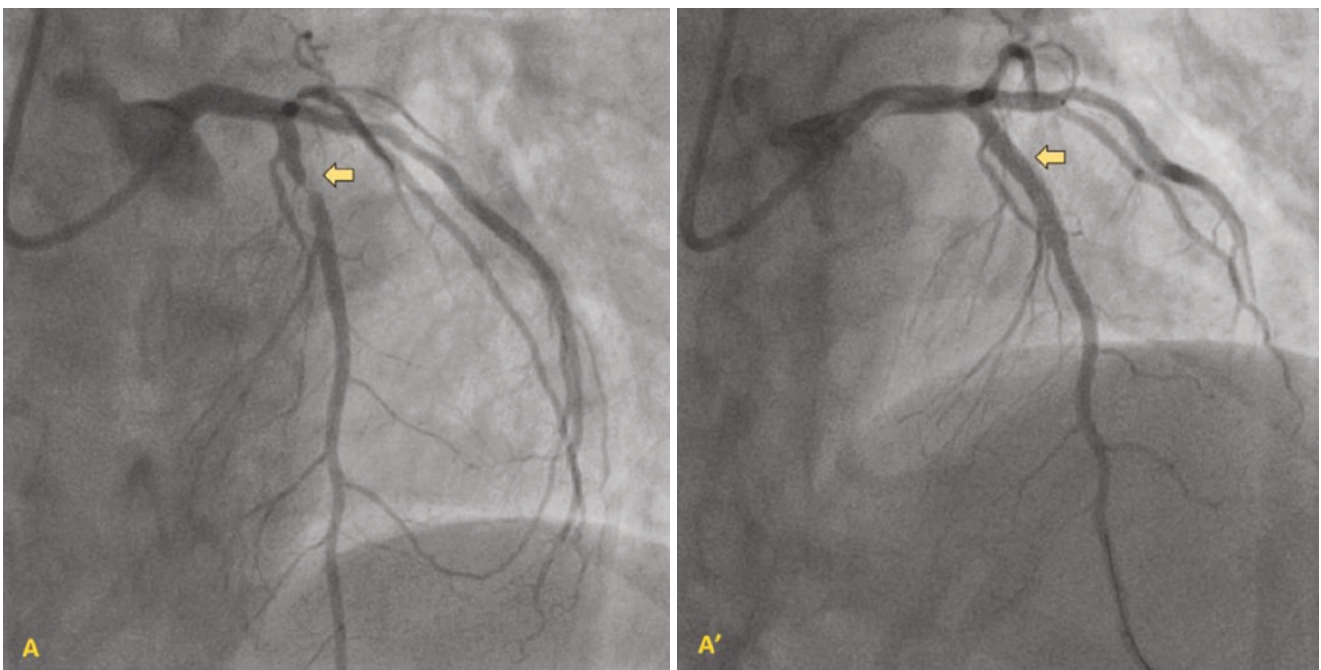


Fig. 1.11 A tight proximal left anterior descending (LAD) artery lesion before (a) and after (a') percutaneous coronary intervention

right shunt, severe valvular disease such as mitral valve disease, pulmonary hypertension) prior to corrective or other surgery.

Direct measurements of the following can be obtained from an accurately placed PAC: Central venous pressure (CVP), right-sided intracardiac pressures (right atrium [RA], right ventricle [RV]), pulmonary arterial pressure (PAP),

pulmonary capillary wedge pressure (PCWP) and mixed venous oxyhemoglobin saturation (SvO_2).

The PAC can also indirectly measure the following: Cardiac output (CO), cardiac index ($CI = CO/\text{body surface area}$), systemic vascular resistance ($SVR = 80 \times [\text{mean arterial pressure} - CVP]/CO$), and pulmonary vascular resistance ($PVR = 80 \times [\text{mean PAP} - PCWP]/CO$).

Procedure

Access is obtained either from the common femoral vein or the forearm, basilic, cephalic or median cubital vein of the arm. Most commonly the catheters used to perform a RHC are multipurpose and Swan-Ganz (5 Fr or 7 Fr sheath) which has an inflatable balloon on its tip and generally safer to use [11].

Complications

Complications are rare but these can be life threatening including RV/RA chamber perforation followed on by tamponade or distal pulmonary artery perforation (which carries a 40–70% mortality and requires often emergency thoracotomy) [25]. Less sinister complications include access site hematomas, arrhythmias, pulmonary infarction, thromboembolism or stroke—in the presence of patent atrioseptal defect or patent foramen ovale.

Interpreting Haemodynamics

Pressure waveforms are obtained in various locations including the RA, RV and PA and its terminal branches.

Right Atrium

The normal waveforms include:

- a wave: contraction of the atria, x descent is the drop in RA pressure following the contraction
- c wave: represents the closure of the tricuspid valve
- v wave: ventricular systole alongside the passive atrial filling, followed by the y descent which represents the opening of the tricuspid valve

Cannon/giant a waves can be seen in any cause of atrioventricular (AV) dissociation (complete heart block, V-paced rhythm, ventricular tachycardia, AV nodal tachycardia etc.). In atrial fibrillation a-waves are absent [26].

Normal RA pressures range from 0 to 7 mmHg. These can be elevated in

- Conditions that cause downstream pressure elevation (pulmonary hypertension, pulmonary valve stenosis),
- Volume/pressure overload due left to right shunts,
- RV dysfunction (cardiomyopathies including restrictive, infarction)
- Tricuspid valve disease (regurgitation causing tall v-waves – even cv waves, and stenosis cannon a waves)
- External compression (tamponade, constrictive pericarditis).

Right Ventricle

Normal RV systolic pressure varies from 15 to 25 mmHg and normal RV end diastolic pressure (RVEDP) from 3 to 12 mmHg. The RV diastolic wave form consists of early rapid filling (60% of filling), slow filling phase (25% of filling) and an atrial systolic phase (a-wave in RV trace).

RV systolic pressures are elevated when there is increased afterload (e.g., pulmonary hypertension, massive pulmonary embolism, pulmonary stenosis). Elevations in RVEDP occur when RV is failing (longstanding pulmonary hypertension, cardiomyopathies affecting RV, RV infarction), external compression (constriction, tamponade).

Pulmonary Artery

Normal PA systolic pressures range from 15 to 25 mmHg while PA diastolic pressures from 8 to 15 mmHg. Mean PA pressures vary from 10 to 22 mmHg (typically around 16 mmHg). Pulmonary hypertension is defined as a mean PA pressure \geq 25 mmHg.

The etiology of pulmonary hypertension is split in the following 5 categories:

1. Pulmonary arterial hypertension (e.g., idiopathic, connective tissue disease, congenital heart disease).
2. Left heart disease (e.g., left heart failure, mitral valvular disease).
3. Chronic lung disease and/or hypoxemia (e.g., emphysema, interstitial lung disease).
4. Chronic pulmonary thromboembolism.
5. Multifactorial mechanisms (e.g., sickle cell disease).

Transient elevations in PA can occur in massive/submassive pulmonary embolism, hypoxia.

Pulmonary Capillary Wedge Pressure

The PCWP is an estimate of the left atrial pressure (LA). This is obtained by inflating the balloon tip of the Swan-Ganz catheter in the distal capillary thus creating a static column of blood between the catheter tip and the left atrium [11]. Normal PCWP varies from 6 to 15 mmHg with a mean of 9 mmHg.

Elevations in PCWP pressure occur in any condition that elevates LA or LV pressures like LV systolic and diastolic failure, mitral and aortic valve disease, cardiac tamponade, constrictive or restrictive cardiomyopathies. Low PCWP can be seen in hypovolemia, pulmonary veno-occlusive disease and obstructive shock due to large pulmonary embolism [27, 28].

PCWP (as RA) has a, c and v waves as well as x and y descents. Large a waves can be seen in mitral stenosis, LV systolic or diastolic dysfunction. Large v waves can be seen traditionally in severe mitral regurgitation, but also in diastolic LV dysfunction (caused by longstanding hypertension, hypertrophic cardiomyopathy, myocardial infarction) [29].

Cardiac output (CO) can be measured either using the indicator thermodilution or the Fick method [30]. Cardiac index is derived from CO divided by the body surface area (BSA). Normal values for CI are 2.8–4.2 L/min/m². Low CO and CI can be seen in LV failure (systolic or diastolic), RV systolic failure, severe mitral regurgitation, pulmonary hypertension and hypovolemia.

Detection of left to right shunts: in the presence of a shunt blood would naturally flow from the higher pressured left chambers to the right corresponding ones. By sampling all the way from superior vena cava, inferior vena cava, RA (high, mid, low), RV and PA the operator can pick up the location of the step up in the oxygen saturation SaO₂ (typically >10% rise) compared to mixed venous SaO₂. Mixed venous SaO₂ is calculated as (3xSVC + IVC)/4 [31]. The degree of the shunting can then be calculated using the ratio of pulmonary flow (Q_p) to systemic flow (Q_s) as shown below.

$$Q_p / Q_s = \text{SAO}_2 - \text{SMVO}_2 / \text{SPVO}_2 - \text{SPAO}_2$$

where: SAO₂ is arterial (aortic) saturation, SMVO₂ is mixed venous saturation, SPVO₂ is pulmonary vein saturation, and SPAO₂ is pulmonary artery saturation.

Finally, the calculation of systemic and pulmonary vascular resistance can be estimated from CO using the Ohm's law (Resistance = Pressure/Flow):

$$\text{SVR} = 80 \times (\text{mean arterial pressure} - \text{RA}) / \text{CO}$$

$$\text{PVR} = 80 \times (\text{mean PA} - \text{PCWP}) / \text{CO}$$

Conclusion

The standard coronary angiography, despite its invasive character and the drawback of relying on a limited number of subjectively selected 2D acquisitions, remains the gold standard method for the evaluation of patients with coronary artery disease. However, several softwares have been developed that permit online co-registration of intravascular imaging, hemodynamic indices and angiographic data. These systems provide representation of coronary angiography, combined with details about lesion morphology and plaque composition, as given by intravascular imaging modalities such as intravascular ultrasound and optical computed tomography [32, 33]. While these approaches have still application mainly in the field of research, the role of standard coronary angiography and right heart catheterization in everyday clinical practice remains fundamental.

References

- Bertrand ME, Meier B. A history of cardiac catheterization. The PCR-EAPCI Textbook. Available at <https://www.pcronline.com/eurointervention/textbook/pcr-textbook/>.
- Judkins MP. Selective coronary arteriography. I. A percutaneous transfemoral technic. *Radiology*. 1967;89:815–24.
- Hurst JW. The first coronary angioplasty as described by Andreas Gruentzig. *Am J Cardiol*. 1986;57:185–6.
- Lozner EC, Johnson LW, Johnson S, Krone R, Pichard AD, Vetrovec GW, et al. Coronary arteriography 1984–1987: a report of the registry of the society for cardiac angiography and interventions. II. An analysis of 218 deaths related to coronary arteriography. *Catheter Cardiovasc Diagn*. 1989;17:11–4.
- Johnson LW, Krone R. Cardiac catheterization 1991: a report of the registry of the society for cardiac angiography and interventions (SCA&I). *Catheter Cardiovasc Diagn*. 1993;28:219–20.
- Ibanez B, James S, Agewall S, Antunes MJ, Bucciarelli-Ducci C, Bueno H, et al. 2017 ESC Guidelines for the management of acute myocardial infarction in patients presenting with ST-segment elevation: The Task Force for the management of acute myocardial infarction in patients presenting with ST-segment elevation of the European Society of Cardiology (ESC). *Eur Heart J*. 2018;39:119–77.
- Neumann FJ, Sousa-Uva M, Ahlsson A, Alfonso F, Banning AP, Benedetto U, et al. 2018 ESC/EACTS Guidelines on myocardial revascularization. *Eur Heart J*. 2018; <https://doi.org/10.1093/eurheartj/ehy394>. [Epub ahead of print].
- Maluenda G, Lemesle G, Collins SD, Ben-Dor I, Syed AI, Torguson R, et al. The clinical significance of hematocrit values before and after percutaneous coronary intervention. *Am Heart J*. 2009;158:1024–30.
- Karjalainen PP, Vikman S, Niemela M, Porela P, Ylitalo A, Vaittinen MA, et al. Safety of percutaneous coronary intervention during uninterrupted oral anticoagulant treatment. *Eur Heart J*. 2008;29:1001–10.
- Ziakas AG, Koskinas KC, Gavriliadis S, Giannoglou GD, Hadjimiliadiades S, Gourassas I, et al. Radial versus femoral access for orally anticoagulated patients. *Catheter Cardiovasc Interv*. 2010;76:493–9.
- Swan HJ, Ganz W, Forrester J, Marcus H, Diamond G, Chonette D. Catheterization of the heart in man with use of a flow-directed balloon-tipped catheter. *N Engl J Med*. 1970;283:447–51.
- Mueller C, Buerkle G, Buettner HJ, Petersen J, Perruchoud AP, Eriksson U, et al. Prevention of contrast media-associated nephropathy: randomized comparison of 2 hydration regimens in 1620 patients undergoing coronary angioplasty. *Arch Intern Med*. 2002;162:329–36.
- Barrett BJ, Parfrey PS. Clinical practice. Preventing nephropathy induced by contrast medium. *N Engl J Med*. 2006;354:379–86.
- Briguori C, Visconti G, Focaccio A, Airolidi F, Valgimigli M, Sangiorgi GM, et al. Renal insufficiency after contrast media administration trial II (REMEDIAL II): RenalGuard System in high-risk patients for contrast-induced acute kidney injury. *Circulation*. 2011;124:1260–9.
- Jolly SS, Yusuf S, Cairns J, Niemela K, Xavier D, Widimsky P, et al. Radial versus femoral access for coronary angiography and intervention in patients with acute coronary syndromes (RIVAL): a randomised, parallel group, multicentre trial. *Lancet*. 2011;377:1409–20.
- Jolly SS, Amlani S, Hamon M, Yusuf S, Mehta SR. Radial versus femoral access for coronary angiography or intervention and the impact on major bleeding and ischemic events: a systematic review and meta-analysis of randomized trials. *Am Heart J*. 2009;157:132–40.
- Heyndrickx GR, Peace AJ, Giris C, Naber CK, Bourantas CV, Serruys PW. Invasive diagnostic coronary angiography. The PCREAPCI Textbook. Available at <https://www.pcronline.com/eurointervention/textbook/pcr-textbook/>.
- Saleem T, Baril DT. Vascular access closure devices. Copyright © 2018: Treasure Island (FL): StatPearls Publishing LLC; 2019.
- Robertson L, Andras A, Colgan F, Jackson R. Vascular closure devices for femoral arterial puncture site haemostasis. *Cochrane Database Syst Rev*. 2016;3:CD009541.
- Kelly AE, Gensini GG. Coronary arteriography and left-heart studies. *Heart Lung*. 1975;4:85–98.

21. Ryan TJ, Faxon DP, Gunnar RM, Kennedy JW, King SB 3rd, Loop FD, et al. Guidelines for percutaneous transluminal coronary angioplasty. A report of the American college of cardiology/American heart association task force on assessment of diagnostic and therapeutic cardiovascular procedures (subcommittee on percutaneous transluminal coronary angioplasty). *Circulation*. 1988;78:486–502.
22. Leaman DM, Brower RW, Meester GT, Serruys P, van den Brand M. Coronary artery atherosclerosis: severity of the disease, severity of angina pectoris and compromised left ventricular function. *Circulation*. 1981;63:285–99.
23. Sianos G, Morel MA, Kappetein AP, Morice MC, Colombo A, Dawkins K, et al. The SYNTAX Score: an angiographic tool grading the complexity of coronary artery disease. *EuroIntervention*. 2005;1:219–27.
24. Farooq V, van Klaveren D, Steyerberg EW, Meliga E, Vergouwe Y, Chieffo A, et al. Anatomical and clinical characteristics to guide decision making between coronary artery bypass surgery and percutaneous coronary intervention for individual patients: development and validation of SYNTAX score II. *Lancet*. 2013;381:639–50.
25. Kearney TJ, Shabot MM. Pulmonary artery rupture associated with the Swan-Ganz catheter. *Chest*. 1995;108:1349–52.
26. Sharkey SW. Beyond the wedge: clinical physiology and the Swan-Ganz catheter. *Am J Med*. 1987;83:111–22.
27. O'Quin R, Marini JJ. Pulmonary artery occlusion pressure: clinical physiology, measurement, and interpretation. *Am Rev Respir Dis*. 1983;128:319–26.
28. Nemens EJ, Woods SL. Normal fluctuations in pulmonary artery and pulmonary capillary wedge pressures in acutely ill patients. *Heart Lung*. 1982;11:393–8.
29. Snyder RW 2nd, Glamann DB, Lange RA, Willard JE, Landau C, Negus BH, et al. Predictive value of prominent pulmonary arterial wedge V waves in assessing the presence and severity of mitral regurgitation. *Am J Cardiol*. 1994;73:568–70.
30. Yelderman ML, Ramsay MA, Quinn MD, Paulsen AW, McKown RC, Gillman PH. Continuous thermodilution cardiac output measurement in intensive care unit patients. *J Cardiothorac Vasc Anesth*. 1992;6:270–4.
31. Flamm MD, Cohn KE, Hancock EW. Measurement of systemic cardiac output at rest and exercise in patients with atrial septal defect. *Am J Cardiol*. 1969;23:258–65.
32. Carlier S, Didday R, Slots T, Kayaert P, Sonck J, El-Mourad M, et al. A new method for real-time co-registration of 3D coronary angiography and intravascular ultrasound or optical coherence tomography. *Cardiovasc Revasc Med*. 2014;15:226–32.
33. Tu S, Holm NR, Koning G, Huang Z, Reiber JH. Fusion of 3D QCA and IVUS/OCT. *Int J Cardiovasc Imaging*. 2011;27:197–207.

Fractional Flow Reserve

2

Vasileios F. Panoulas

High Yield Facts

- Visual angiographic stenosis assessment is a poor predictor of the functional significance of a stenosis.
- Sensor tipped angioplasty guidewires have been developed and are used to measure pressure and flow across a coronary stenosis in the catheterization laboratory.
- A normal fractional flow reserve (FFR) value is 1, while a positive test is considered when the FFR <0.80 .
- Dobutamine stress echocardiography has been shown to correlate well with FFR.
- FFR is superior to intravascular ultrasound
- The most common reason to have a false negative FFR (i.e., a falsely high FFR) is guide catheter pressure damping.
- False positive FFR values (falsely low FFR) are the result of technical failures.

emia as demonstrated in prior non-invasive testing. However, commonly the lesions encountered in coronary angiograms are intermediate (Fig. 2.1), with luminal stenosis in the range of 40–80% diameter reduction [1, 2]. In this subtype of lesions coronary artery physiologic data, usually coronary artery pressure and flow, can aid decision on the need for revascularization, particularly in individuals without prior non-invasive stress test. Furthermore, visual estimation of stenosis severity has been shown to be highly variable between different operators (inter-observer) but also in repeated assessments (intra-observer) [3]. Visual angiographic stenosis assessment is a poor predictor of the functional significance of a stenosis.

Sensor tipped angioplasty guidewires have been developed and are used to measure pressure and flow across a coronary stenosis in the catheterization laboratory [4, 5]. The use of coronary pressure guidewires is generally safe and typically adds a few minutes to the total procedure time for the assessment of each lesion.

Introduction

Myocardial revascularization with either percutaneous coronary intervention (PCI) or coronary artery bypass grafting (CABG) is indicated in the presence of significant ischaemia in one or more coronary territories. In most cases, coronary artery stenoses with greater than 80% diameter reduction on coronary angiography are associated with myocardial isch-

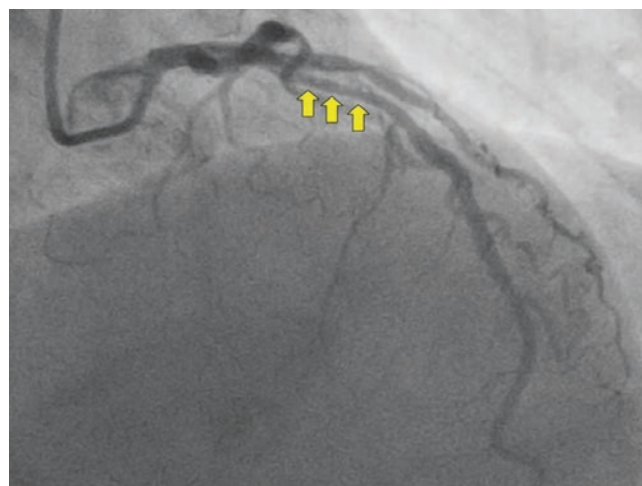


Fig. 2.1 Intermediate lesion on coronary angiography indicated by arrows

V. F. Panoulas (✉)
Royal Brompton and Harefield NHS Foundation Trust,
Harefield, UK

National Heart and Lung Institute, Imperial College London,
London, UK
e-mail: v.panoulas@imperial.ac.uk

Definitions

Fractional flow reserve (FFR) is the ratio of the maximum achievable blood flow to a myocardial territory in the presence of a stenosis to the maximum achievable flow to the same territory in the absence of the stenosis [6] (Fig. 2.2).

$$FFR = \frac{Q_S}{Q_N} = \frac{P_d - P_v}{P_a - P_v} \frac{R_{myoN}}{R_{myoS}}$$

Where

- Q_S is the maximum achievable flow to the territory supplied by the epicardial vessel with stenosis in question.
- Q_N is the maximum achievable flow to the same territory presuming the epicardial vessel is normal.

- P_d is the pressure measured at the guidewire pressure sensor which should be positioned distal to the lesion in question and
- P_a is the aortic pressure which is the pressure measured at the tip of the guide catheter.
- P_v is the central venous pressure which is much lower than P_a , P_d and close to zero
- R_{myoS} is the myocardial resistance in the territory supplied by the stenosed vessel
- R_{myoN} is the myocardial resistance in the territory supplied by the same vessel with no coronary artery stenoses

If we consider

- The central venous pressure $P_v = 0$ and
- $R_{myoS} = R_{myoN}$

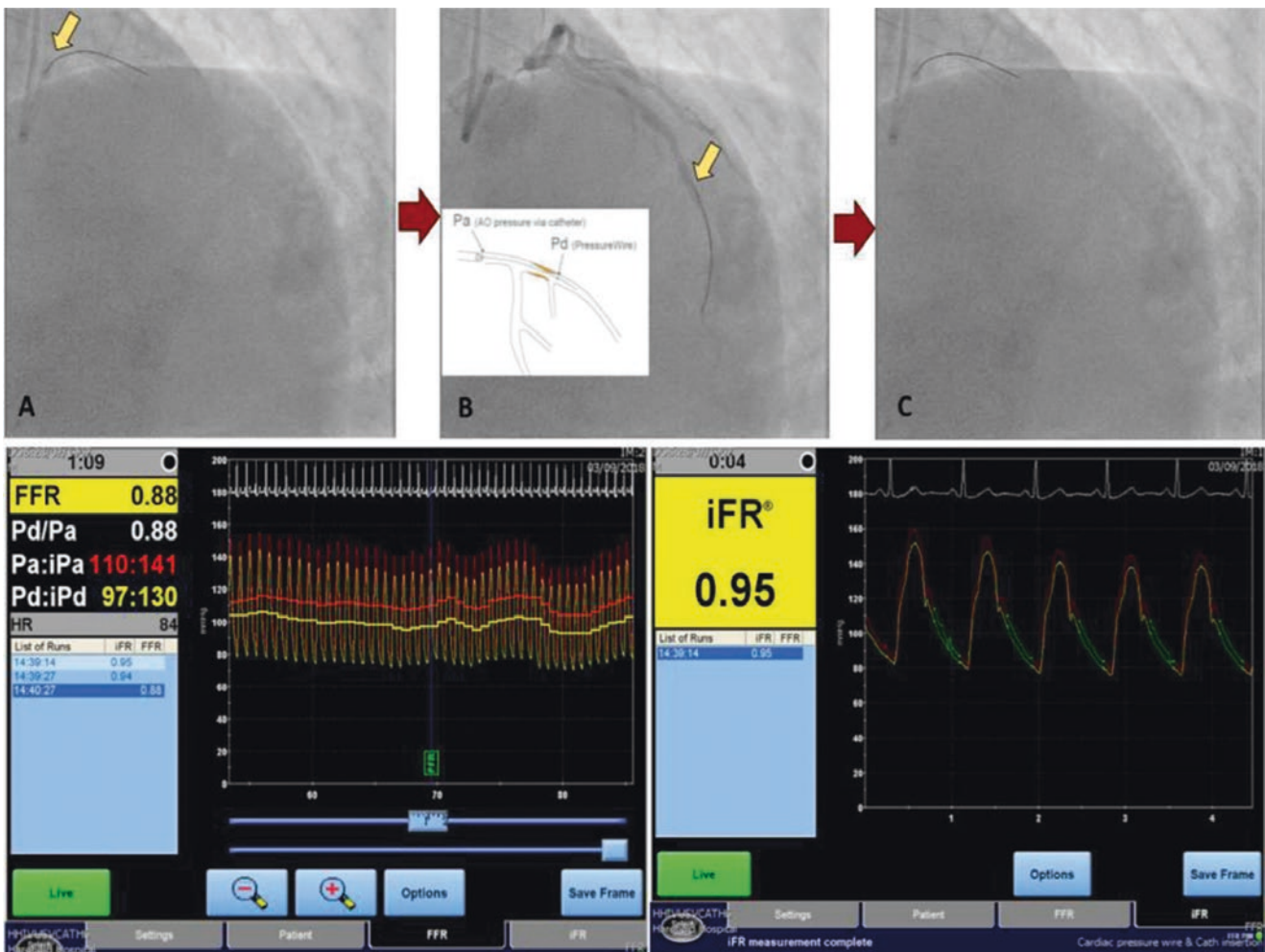


Fig. 2.2 Determination of fractional flow reserve (FFR) and instantaneous wave-free pressure ratio (iFR)

then the equation can be simplified to:

$$FFR = \frac{Pd}{Pa}$$

To obtain accurate FFR measurements, pressures obtained during hyperaemia are required. Maximal blood flow (hyperaemia) is most commonly induced by intravenous (140 mcg/kg/min) or intracoronary adenosine (right coronary artery 50–100 mcg, left coronary artery 100–200 mcg bolus). A normal FFR value is 1, while a positive test is considered when the FFR <0.80.

How Was This Cut-Off Decided?

In a seminal paper by Pijls et al. [7] FFR was compared to exercise testing, thallium scintigraphy, dobutamine stress echocardiography (DSE) and quantitative arteriography in 45 consecutive patients with moderate coronary stenosis and chest pain, prospectively testing the cut-off value of 0.75 [8] to a true gold standard based upon the combination of the three non-invasive tests, all performed within 24 h from the FFR measurement. Using multi-testing sequential Bayesian approach, the sensitivity of FFR in the identification of reversible ischemia was 88%, the specificity 100%, the positive predictive value 100%, and the negative predictive value 88%. In order to avoid not treating an ischemic lesion than treating a non-ischemic lesion, in the FAME [9] and FAME 2 [10] trials a cut-off value of 0.80 was used, demonstrating the prognostic benefits of FFR guided revascularization. In a more recent retrospective study, in an attempt to justify the use of the 0.80 cut-off in clinical practice, Adjedj et al. [11] investigated the outcomes of patients with single lesions in the so called “grey zone” or FFR 0.76–0.80 who were either revascularised or treated with medical therapy alone. Of interest, even though there was no significant difference in overall major adverse cardiovascular events (MACE), there was a trend for higher mortality ($p = 0.059$) and the combined outcome of myocardial infarction (MI)/death ($p = 0.06$) in the medical therapy group.

FFR Compared to Other Non-invasive Diagnostic Techniques

DSE has been shown to correlate well with FFR (cut off 0.8) in a study of 62 patients with a single intermediate angiographic lesion with kappa 0.682 and a diagnostic agreement in 87% of patients [12].

Magnetic resonance myocardial perfusion imaging (MRMPI), with intravenous adenosine and a first-pass gadolinium bolus, has been shown to correlate well with FFR (using a cut off at 0.75) in detecting reversible ischemia in a study of 103 patients with stable angina (300 coronary artery segments), MRMPI had a high sensitivity 91%, specificity 94%, positive predictive value 91% and negative predictive value 94% for detecting functionally significant coronary stenosis [13]. In a similar study, of 42 patients who had undergone quantitative stress cardiac magnetic resonance imaging (cMRI) 52 lesions were pressure wired and a cut off of 0.75 was chosen to determine significance. Sensitivity and specificity of cMR to detect haemodynamically significant lesions were 82% and 94% respectively whereas optimum myocardial perfusion reserve (MPR) was 1.58 [14].

Dipyridamole technetium-99m sestamibi (MIBI) single-photon emission computed tomography (SPECT) appears to correlate modestly with FFR in a study of 127 patients (161 coronary lesions) with a 77% diagnostic agreement with FFR and a modest kappa of 0.47 [15].

Single-photon emission computed tomography (PET-CT) myocardial perfusion imaging showed poor correlation with FFR in identifying ischemic territories in patients with multivessel disease, in a study of 67 patients (201 vascular territories) with angiographic 2- or 3-vessel coronary artery disease. The two modalities detected identical ischemic territories in only 42% of patients with kappa of 0.14 (–10 to 0.39) [16].

Adenosine stress computed tomography myocardial perfusion imaging (CTP) showed a moderate correlation with FFR in a study of 42 patients (126 vessels) with at least one >50% angiographic stenosis [17]. CTP achieved 76% diagnostic accuracy in ischaemic lesions and 84% in non-ischaemic territories (Table 2.1).

Table 2.1 Diagnostic indices of non-invasive modalities using FFR as gold standard

	Sensitivity (%)	Specificity (%)	PPV (%)	NPV (%)
DSE [12]	60	87.5	100	83.8
Stress cMRI [13]	91	94	91	94
PET-CT [16]	76	38	66	50
CT perfusion [17]	76	84	82	79
MIBI [15]	83	66		

DSE dobutamine stress echocardiography, cMRI cardiac magnetic resonance imaging, CT computed tomography, MIBI dipyridamole technetium-99m sestamibi, NPV negative predictive value, PET-CT Single-photon emission computed tomography, PPV positive predictive value

Limitations of Pressure Wire Measurements

The most common reason to have a false negative FFR (i.e., a falsely high FFR) is guide catheter pressure damping (preventing flow into the vessel), failure to induce hyperaemia (wrong concentration, poor intravenous infusion), or acute coronary syndrome with an impaired myocardial bed acutely that then improves over time.

False positive FFR values (falsely low FFR) are the result of technical failures due to inaccurate calibrations, guidewire signal drift downward, or aortic pressure drift upward.

In addition to obstructive focal lesions, flow to the myocardium can be impaired by the presence of diffuse atherosclerotic disease or microcirculatory dysfunction. Other measurements of coronary flow, such as the coronary flow reserve and the index of microcirculatory resistance, have been evaluated as tools for assessing the microcirculation [18]. The role of these measures in clinical practice has not been established.

Intravascular Ultrasound and FFR

Intravascular ultrasound (IVUS), a standard for intravascular anatomic information, has attempted to establish a physiologic correlation to anatomic dimensions. In a prospective registry of 350 patients with 367 intermediate coronary lesions (40–80% by angiography), anatomic measurements by IVUS showed only a moderate correlation with FFR values [19]. The cross-sectional lumen area (i.e., minimal luminal area or MLA) measured by these techniques has been proposed as a surrogate measurement of the functional significance of a given stenosis, however the correlation with FFR has been only moderate. Overall an MLA < 3.07 mm² (64.0% sensitivity, 64.9% specificity, AUC = 0.65) was the best threshold value for identifying FFR < 0.8. The accuracy improved when reference vessel-specific analyses were performed. An MLA < 2.4 mm² (AUC = 0.66) was best for reference vessel diameters < 3.0 mm, an MLA < 2.7 mm² (AUC = 0.71) for reference vessel diameters of 3.0–3.5 mm, and an MLA < 3.6 mm² (AUC = 0.68) for reference vessel diameters > 3.5 mm. FFR correlated with plaque burden ($r = -0.220$, $p < 0.001$) but not with other plaque morphology.

Assessing Left Main Stem Stenosis Using FFR

The left main stem (LMS) stenosis is among the most difficult lesions to interpret angiographically and among the most critical of clinical presentations. LMS stenosis may involve the aortic-ostial junction, mid-body, or distal segments, which may involve the left anterior descending (LAD)/circumflex ostia. When assessing ostial LMS narrowing by fractional

flow reserve (FFR), care is needed to avoid guide catheter damping by disengaging the guide from the ostium and using intravenous adenosine to achieve consistent hyperaemia. In case of a distal narrowing of the LMS, this procedure may be performed twice, once with the pressure wire in the LAD artery and then again in the circumflex artery.

Numerous studies support FFR for assessment of LMS stenoses. In the largest study [20], five-year outcomes were examined in 213 patients with an angiographically equivocal LMS stenosis in whom revascularization decisions were guided by FFR. When FFR was ≥ 0.80 , patients were treated medically or another stenosis was treated by coronary angioplasty (nonsurgical group; $n = 138$). When FFR was < 0.80, CABG was performed (surgical group; $n = 75$). The five-year survival and event-free survival rates were similar with 90 and 74% in the nonsurgical (FFR ≥ 0.80) group and 85 and 82% in the surgical (FFR < 0.80) group ($p = 0.48$). Of note only 23% of patients with LMS > 50% diameter stenosis had a hemodynamically significant FFR.

FFR in LMS lesions with downstream disease (e.g., LAD lesions) requires an understanding of serial lesions and how they affect one another. The myocardial bed flow for the LMS is the sum of both the LAD and circumflex territories and this flow determines the LMS FFR. In the presence of a significant LAD stenosis, flow in the LAD territory may be reduced, reducing total LMS flow and hence falsely increasing the apparent LMS FFR value. The higher “apparent” LMS FFR is only a concern if either the LAD or circumflex, are severely hemodynamically impaired (FFR of LMS and LAD < 0.6) [21]. For serial LMS with downstream LAD disease, when FFR beyond LAD is < 0.60, the apparent LMS FFR may be questioned. In this case, IVUS assessment with a threshold of < 6.0 mm² is recommended.

FFR Use Pre Coronary Artery Bypass Grafting

The issue of whether the use of FFR to evaluate intermediate lesions can improve outcomes in patients referred for CABG has been evaluated in one observational study [22]. Among 627 patients having at least one angiographically intermediate stenosis, 429 had bypass grafts placed based on angiographic findings only, and 198 based on FFR (bypass of a lesion was deferred if the FFR was > 0.80). At 3 years, major adverse cardiovascular events (a composite of overall death, MI, and target vessel revascularization) were similar between the two groups (12% versus 11%; HR 1.03, 95% CI 0.67–1.69). The rate of angina was significantly lower in the FFR-guided group (31% versus 47%), despite fewer venous grafts being placed.

While the surgical practice of grafting all vessels with angiographic stenosis of > 50% has been a long-standing standard, CABG of vessels with haemodynamically non-

significant stenosis has a higher rate of graft closure compared with those vessels with haemodynamically significant stenosis [23]. This was shown in 525 lesions in 153 patients referred for bypass surgery. FFR was performed in all lesions to be grafted, with the surgeon blinded to the results. Repeat angiogram performed one year after CABG showed that 21.4% of grafts on functionally non-significant lesions (FFR >0.75) were occluded, compared with 8.9% of grafts on vessels with FFR <0.75.

Main Outcome Studies with FFR

DEFER Trial [24]

In 325 patients scheduled for PCI of an intermediate stenosis, FFR was measured just before the planned intervention. If FFR was ≥ 0.75 , patients were randomly assigned to defer (Defer group; $n = 91$) or performance (Perform group; $n = 90$) of PCI. If FFR was <0.75, PCI was performed as planned (Reference group; $n = 144$). After 15 years of clinical follow up the rate of death was not different between the three groups: 33.0% in the Defer group, 31.1% in the Perform group, and 36.1% in the Reference group (Defer vs. Perform, RR 1.06, 95% CI: 0.69–1.62, $P = 0.79$). The rate of myocardial infarction was significantly lower in the Defer group (2.2%) compared with the Perform group (10.0%) [RR 0.22, 95% CI: 0.05–0.99, $P = 0.03$].

FAME Trial [9]

In the FAME study, 1005 patients with multivessel coronary artery disease were randomly assigned to undergo PCI with implantation of drug-eluting stents guided by angiography alone or guided by FFR measurements in addition to angiography. The primary end point was the rate of death, nonfatal MI, and repeat revascularization at 1 year. The 1-year event rate was 18.3% (91 patients) in the angiography group and 13.2% (67 patients) in the FFR group ($P = 0.02$). All-cause mortality at 1 year was 3.0% (15 deaths, 10 of which had cardiac causes) in the angiography group and 1.8% (9 deaths, 7 of which had cardiac causes) in the FFR group ($P = 0.19$). MI occurred in 43 patients (8.7%) in the angiography group and in 29 (5.7%) in the FFR group ($P = 0.07$). Repeat revascularization occurred in 47 patients (9.5%) in the angiography group and 33 (6.5%) in the FFR group, $p = 0.08$. At 5-years major adverse cardiac events occurred in 31% of patients (154 of 496) in the angiography-guided group versus 28% (143 of 509 patients) in the FFR-guided group (relative risk 0.91, 95% CI 0.75–1.10; $p = 0.31$) [25].

FAME 2 Trial [10]

In 1220 stable angina patients with angiographically significant stenosis, those in whom at least one stenosis was hemodynamically significant (FFR ≤ 0.80) were randomly assigned to FFR-guided PCI plus medical therapy or to medical therapy alone. Patients in whom all stenoses had an FFR of more than 0.80 received medical therapy and were entered into a registry. The primary end point was a composite of death, MI, or urgent revascularization. A total of 888 patients underwent randomization (447 patients in the PCI group and 441 in the medical-therapy group). At 5 years, the rate of the primary end point was lower in the PCI group than in the medical-therapy group (13.9% vs. 27.0%; hazard ratio, 0.46; 95% confidence interval [CI], 0.34–0.63; $P < 0.001$) [26]. The difference was driven by urgent revascularizations, which occurred in 6.3% of the patients in the PCI group as compared with 21.1% of those in the medical-therapy group (hazard ratio, 0.27; 95% CI, 0.18–0.41). There were no significant differences between the PCI group and the medical-therapy group in the rates of death (5.1% and 5.2%, respectively; hazard ratio, 0.98; 95% CI, 0.55–1.75) or MI (8.1% and 12.0%; hazard ratio, 0.66; 95% CI, 0.43–1.00) [26].

COMPARE ACUTE Trial [27]

In this study 885 patients with ST elevation MI and multivessel disease who had undergone primary PCI of an infarct-related coronary artery were randomly assigned in a 1:2 ratio to undergo complete revascularization of non-infarct-related coronary arteries guided by fractional flow reserve (FFR) (295 patients) or to undergo no revascularization of non-infarct-related coronary arteries (590 patients). The FFR procedure was performed in both groups, but in the latter group, both the patients and their cardiologist were unaware of the findings on FFR. The primary end point was a composite of death from any cause, nonfatal MI, revascularization, and cerebrovascular events at 12 months. The primary outcome occurred in 8% of patients in the complete-revascularization group and 21% of patients in the infarct-artery-only group that did not receive complete revascularization (HR, 0.35; 95%CI, 0.22 to 0.55; $P < 0.001$). Death occurred in 4 patients in the complete-revascularization group and in 10 patients in the infarct-artery-only group (1.4% vs. 1.7%) (HR, 0.80; 95%CI, 0.25–2.56), MI in 7 and 28 patients, respectively (2.4% vs. 4.7%) (HR, 0.50; 95% CI, 0.22–1.13), revascularization in 18 and 103 patients (6.1% vs. 17.5%) (HR, 0.32; 95%CI, 0.20–0.54), and cerebrovascular events in 0 and 4 patients (0 vs. 0.7%) [27].

Instantaneous Wave-Free Pressure Ratio (iFR)

An adenosine-independent, resting pressure-derived index of coronary stenosis severity has been developed and tested as a substitute for FFR. Using wave intensity analysis [28], it was determined that the period of diastole in which equilibration or balance between pressure waves from the aorta and distal microcirculatory reflection was a “wave-free period” led to minimal and constant coronary resistance. Pd/Pa during the wave-free period (75% into diastole ending 5 ms before the R wave) is called the instantaneous wave-free pressure ratio (iFR) (Fig. 2.2).

It was demonstrated that at iFR cut off-points of >0.93 or <0.86 , there was a strong correlation with normal and abnormal FFR values respectively (using 0.80 as an FFR cut point). In the ADVISE II study [29], iFR was compared to FFR in 690 intermediate stenoses. Compared to FFR (using the 0.80 cut off point), iFR cut-off of 0.89 correctly classified 83% of stenoses. iFR correctly classified those stenoses outside the 0.85–0.94 iFR “gray zone” with 92% agreement.

Two large randomized, non-inferiority trials in low-risk patients have evaluated clinical outcomes in patients with stable or unstable disease who had one or more coronary artery lesions for which physiologic assessment prior to revascularization was indicated; In the iFR SWEDEHEART study, 2037 patients were randomly assigned to iFR (cut off 0.89) or FFR (cut off 0.8) [30]. The primary end point (all cause death from, nonfatal MI, or unplanned revascularization within 12 months) occurred with equal frequency (6.7% versus 6.1%; difference in event rates, 0.7 percentage points, 95% CI -1.5 to 2.8 ; HR 1.12, 95% CI 0.79–1.58). In the DEFINE-FLAIR trial, 2492 patients were randomly assigned to iFR or FFR [31]. At one year, the primary end point, a composite of death from any cause, nonfatal MI, or unplanned revascularization, occurred with equal frequency (6.8% versus 7.0%; difference in risk, -0.2 percentage points; 95% CI, -2.3 to 1.8 ; $P < 0.001$ for noninferiority; HR, 0.95; 95% CI, 0.68–1.33; $P = 0.78$).

Conclusions

FFR has become the clinical standard for the invasive physiologic assessment of the hemodynamic significance of intermediate stenoses. FFR is superior to intravascular ultrasound and in many cases to noninvasive stress radionuclide myocardial perfusion imaging. For intermediate stenoses where there is a question of whether revascularization should be carried out, with no prior noninvasive physiologic data to guide decision making, FFR should always be measured before the decision to revascularize.

References

1. Kern MJ, Samady H. Current concepts of integrated coronary physiology in the catheterization laboratory. *J Am Coll Cardiol.* 2010;55:173–85.
2. White CW, Wright CB, Doty DB, et al. Does visual interpretation of the coronary arteriogram predict the physiologic importance of a coronary stenosis? *N Engl J Med.* 1984;310:819–24.
3. Beauman GJ, Vogel RA. Accuracy of individual and panel visual interpretations of coronary arteriograms: implications for clinical decisions. *J Am Coll Cardiol.* 1990;16:108–13.
4. Qian J, Ge J, Baumgart D, et al. Safety of intracoronary Doppler flow measurement. *Am Heart J.* 2000;140:502–10.
5. Donohue TJ, Kern MJ, Aguirre FV, et al. Assessing the hemodynamic significance of coronary artery stenoses: analysis of translational pressure-flow velocity relations in patients. *J Am Coll Cardiol.* 1993;22:449–58.
6. Gould KL, Lipscomb K. Effects of coronary stenoses on coronary flow reserve and resistance. *Am J Cardiol.* 1974;34:48–55.
7. Pijls NH, De Bruyne B, Peels K, et al. Measurement of fractional flow reserve to assess the functional severity of coronary-artery stenoses. *N Engl J Med.* 1996;334:1703–8.
8. Pijls NH, Van Gelder B, Van der Voort P, et al. Fractional flow reserve. A useful index to evaluate the influence of an epicardial coronary stenosis on myocardial blood flow. *Circulation.* 1995;92:3183–93.
9. Tonino PA, De Bruyne B, Pijls NH, et al. Fractional flow reserve versus angiography for guiding percutaneous coronary intervention. *N Engl J Med.* 2009;360:213–24.
10. De Bruyne B, Pijls NH, Kalesan B, et al. Fractional flow reserve-guided PCI versus medical therapy in stable coronary disease. *N Engl J Med.* 2012;367:991–1001.
11. Adedj J, De Bruyne B, Flore V, et al. Significance of intermediate values of fractional flow reserve in patients with coronary artery disease. *Circulation.* 2016;133:502–8.
12. Panoulas VF, Keramida K, Boletti O, et al. Association between fractional flow reserve, instantaneous wave-free ratio and dobutamine stress echocardiography in patients with stable coronary artery disease. *EuroIntervention.* 2018;13:1959–66.
13. Watkins S, McGeoch R, Lyne J, et al. Validation of magnetic resonance myocardial perfusion imaging with fractional flow reserve for the detection of significant coronary heart disease. *Circulation.* 2009;120:2207–13.
14. Lockie T, Ishida M, Perera D, et al. High-resolution magnetic resonance myocardial perfusion imaging at 3.0-Tesla to detect hemodynamically significant coronary stenoses as determined by fractional flow reserve. *J Am Coll Cardiol.* 2011;57:70–5.
15. Chamuleau SA, Meuwissen M, van Eck-Smit BL, et al. Fractional flow reserve, absolute and relative coronary blood flow velocity reserve in relation to the results of technetium-99m sestamibi single-photon emission computed tomography in patients with two-vessel coronary artery disease. *J Am Coll Cardiol.* 2001;37:1316–22.
16. Melikian N, De Bondt P, Tonino P, et al. Fractional flow reserve and myocardial perfusion imaging in patients with angiographic multivessel coronary artery disease. *JACC Cardiovasc Interv.* 2010;3:307–14.
17. Ko BS, Cameron JD, Meredith IT, et al. Computed tomography stress myocardial perfusion imaging in patients considered for revascularization: a comparison with fractional flow reserve. *Eur Heart J.* 2012;33:67–77.
18. Echavarría-Pinto M, Escaned J, Macías E, et al. Disturbed coronary hemodynamics in vessels with intermediate stenoses evaluated with fractional flow reserve: a combined analysis of epicardial and microcirculatory involvement in ischemic heart disease. *Circulation.* 2013;128:2557–66.

19. Waksman R, Legutko J, Singh J, et al. FIRST: fractional flow reserve and intravascular ultrasound relationship study. *J Am Coll Cardiol*. 2013;61:917–23.
20. Hamilos M, Muller O, Cuisset T, et al. Long-term clinical outcome after fractional flow reserve-guided treatment in patients with angiographically equivocal left main coronary artery stenosis. *Circulation*. 2009;120:1505–12.
21. Fearon WF, Yong AS, Lenders G, et al. The impact of downstream coronary stenosis on fractional flow reserve assessment of intermediate left main coronary artery disease: human validation. *JACC Cardiovasc Interv*. 2015;8:398–403.
22. Toth G, De Bruyne B, Casselman F, et al. Fractional flow reserve-guided versus angiography-guided coronary artery bypass graft surgery. *Circulation*. 2013;128:1405–11.
23. Botman CJ, Schonberger J, Koolen S, et al. Does stenosis severity of native vessels influence bypass graft patency? A prospective fractional flow reserve-guided study. *Ann Thorac Surg*. 2007;83:2093–7.
24. Zimmermann FM, Ferrara A, Johnson NP, et al. Deferral vs. performance of percutaneous coronary intervention of functionally non-significant coronary stenosis: 15-year follow-up of the DEFER trial. *Eur Heart J*. 2015;36:3182–8.
25. van Nunen LX, Zimmermann FM, Tonino PA, et al. Fractional flow reserve versus angiography for guidance of PCI in patients with multivessel coronary artery disease (FAME): 5-year follow-up of a randomised controlled trial. *Lancet*. 2015;386:1853–60.
26. Xaplanteris P, Fournier S, Pijls NHJ, et al. Five-year outcomes with PCI guided by fractional flow reserve. *N Engl J Med*. 2018;379:250–9.
27. Smits PC, Boxma-de Klerk BM. Fractional flow reserve-guided multivessel angioplasty in myocardial infarction. *N Engl J Med*. 2017;377:397–8.
28. Sen S, Escaned J, Malik IS, et al. Development and validation of a new adenosine-independent index of stenosis severity from coronary wave-intensity analysis: results of the ADVISE (ADenosine Vasodilator Independent Stenosis Evaluation) study. *J Am Coll Cardiol*. 2012;59:1392–402.
29. Escaned J, Echavarría-Pinto M, García-García HM, et al. Prospective assessment of the diagnostic accuracy of instantaneous wave-free ratio to assess coronary stenosis relevance: results of ADVISE II international, multicenter study (ADenosine vasodilator independent stenosis evaluation II). *JACC Cardiovasc Interv*. 2015;8:824–33.
30. Gotberg M, Christiansen EH, Gudmundsdóttir IJ, et al. Instantaneous wave-free ratio versus fractional flow reserve to guide PCI. *N Engl J Med*. 2017;376:1813–23.
31. Davies JE, Sen S, Dehbi HM, et al. Use of the instantaneous wave-free ratio or fractional flow reserve in PCI. *N Engl J Med*. 2017;376:1824–34.



Echocardiography

3

Shelley Rahman Haley

High Yield Facts

- Echocardiography is the most widely-practiced noninvasive imaging modality and uses ultrasound to build up a detailed anatomical and physiological picture of the heart and great vessels.
- Echocardiography is widely-available, repeatable, reproducible, very low-risk, virtually painless and relatively cheap.
- Different modalities of imaging within the technique allow the identification and accurate assessment of global and regional ventricular systolic and diastolic dysfunction, myocardial viability and ischemia, stenotic and regurgitant valve lesions, pericardial disease and intracardiac masses.
- Data accumulated over almost five decades of practice means that information obtained by echocardiography predicts outcomes of surgical procedures including mitral valve repair, aortic valve replacement, myocardial revascularization and left ventricular assist device implantation.

Introduction

Echocardiography uses ultrasound to build up images of the heart and great vessels. In cardiothoracic surgery in developed economies, it is the most widely-practiced and highest-volume non-invasive diagnostic imaging test performed. The proven utility of the technique along with its low risk-profile mean that it is the cornerstone of cardiac imaging. Entire textbooks are devoted to single modalities of echocardiography, and the interested reader is directed to the bibliography

at the end of this chapter. However, this chapter is intended to provide a brief and focused survey of the technique as it applies to the cardiothoracic surgical patient. A brief section on ultrasound theory is included, containing only the facts deemed to be essential for a basic understanding of the way various measurements are made and parameters calculated. Some formulae are also included in the text where it is felt that this facilitates understanding.

Essential Ultrasound Theory for Echocardiography

The ultrasound used in echocardiography is produced by passing electric current through a piezoelectric crystal, causing it to vibrate at frequencies of 2–7 MHz. The ultrasound waves pass through the tissues of the thorax, and are scattered, attenuated or reflected particularly at tissue interfaces. The reflected signals deform the piezoelectric crystal and generate tiny electric currents which are used to build up a detailed picture of the structure of the heart. The simultaneous recording of the patient's surface ECG allows the images to be gated, transforming them into the real-time cines with which surgeons are most familiar (Fig. 3.1). Doppler echocardiography utilizes the physics of the Doppler frequency shift to allow calculation of the speed of motion of blood through the heart valves and this in turn allows the calculation of valve area/stenosis, cardiac output and regurgitant volume. The attenuation of ultrasound by body tissues means that image quality is affected by body habitus, and some subjects simply have poor acoustic windows, so image quality can never be guaranteed. Nevertheless, with advances in hardware and software, there are few patients in whom useful information cannot be obtained.

S. R. Haley (✉)
Department of Cardiology, Harefield Hospital, London, UK
e-mail: s.rahmanhaley@rbht.nhs.uk

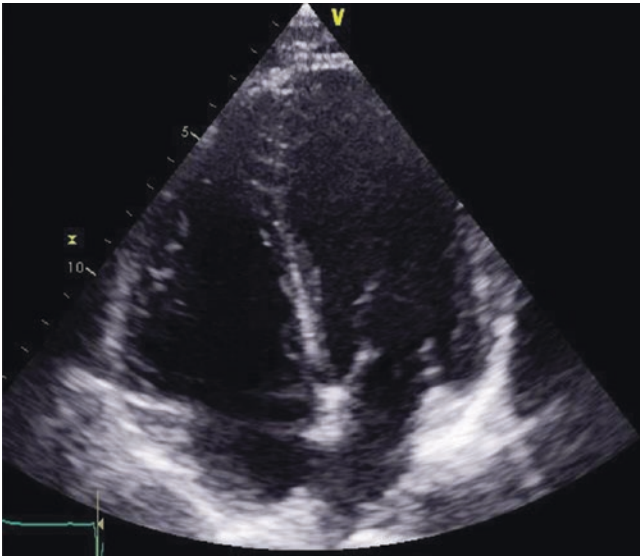


Fig. 3.1 2D 4-chamber view in a patient with a normal heart

Modalities of Echocardiography

In addition to the 2D echo images already mentioned, there are a number of other echo modalities with specific uses and these are summarized in Table 3.1.

Motion-mode (M-mode) has extremely high temporal resolution and is particularly good for situations where an understanding of the relative timing of events is key. An example of this is in the assessment of the hemodynamic significance of a pericardial effusion when the presence of early diastolic collapse of the free wall of the right ventricle is one of the important echo indicators of incipient tamponade [1].

Pulsed-wave (PW) and continuous-wave (CW) Doppler echocardiography are used to assess flow velocity (Fig. 3.2). The former uses a sample-volume to provide information from a particular selected depth, but is only able to assess relatively low flow velocities (up to approximately 1.8 m/s). This is because the transducer acts as a receiver for the time necessary for the signals to return from the sample volume, after which a further pulse is emitted. This in turn means that there is a limit to the sampling rate, and this limits the maximum velocity able to be detected accurately [1]. Continuous wave Doppler is not limited in this way because the transducer acts as a continuous emitter and receiver of ultrasound. However, this modality is not able to provide range resolution.

Color flow Doppler is used to provide an easy, immediately-appreciable visual assessment of blood flow through the chambers and valves. By convention, in areas of the image where blood is flowing towards the transducer it is coded red and when it is flowing away from the transducer it is coded blue. Although color flow mapping allows the

Table 3.1 Modalities of echocardiography and their main uses

Modality of echo	Advantages	Disadvantages	Main uses
2D	Recognizable, moving images	Dependent on acoustic windows and operator	Anatomy and morphology; “eyeballing” function and valve motion
M Mode	Very high temporal resolution	Images harder to interpret for the less experienced observer	Dimensions, accurate timing of motion of structures such as valve leaflets
CW (continuous wave) Doppler	Can be used with 2D and color flow Doppler to measure velocities over a wide range	Not fully steerable so measurements may be less accurate if correct angle cannot be obtained	Measuring velocities across stenotic and regurgitant valves
PW (pulsed wave) Doppler	Sample volume means able to localize velocities at a specific point in the heart	Can only be used to measure velocities up to 2 m/s	Measuring filling parameters, LVOT /RVOT velocity, pulmonary and hepatic venous flow
“Standalone” CW Doppler	Highly steerable allowing accurate measurement of velocities at tricky angles	The operator cannot see the 2D image simultaneously, so harder to use and requires more experience	Valve lesions, accurate assessment of aortic stenosis, separating out complex overlapping velocity traces

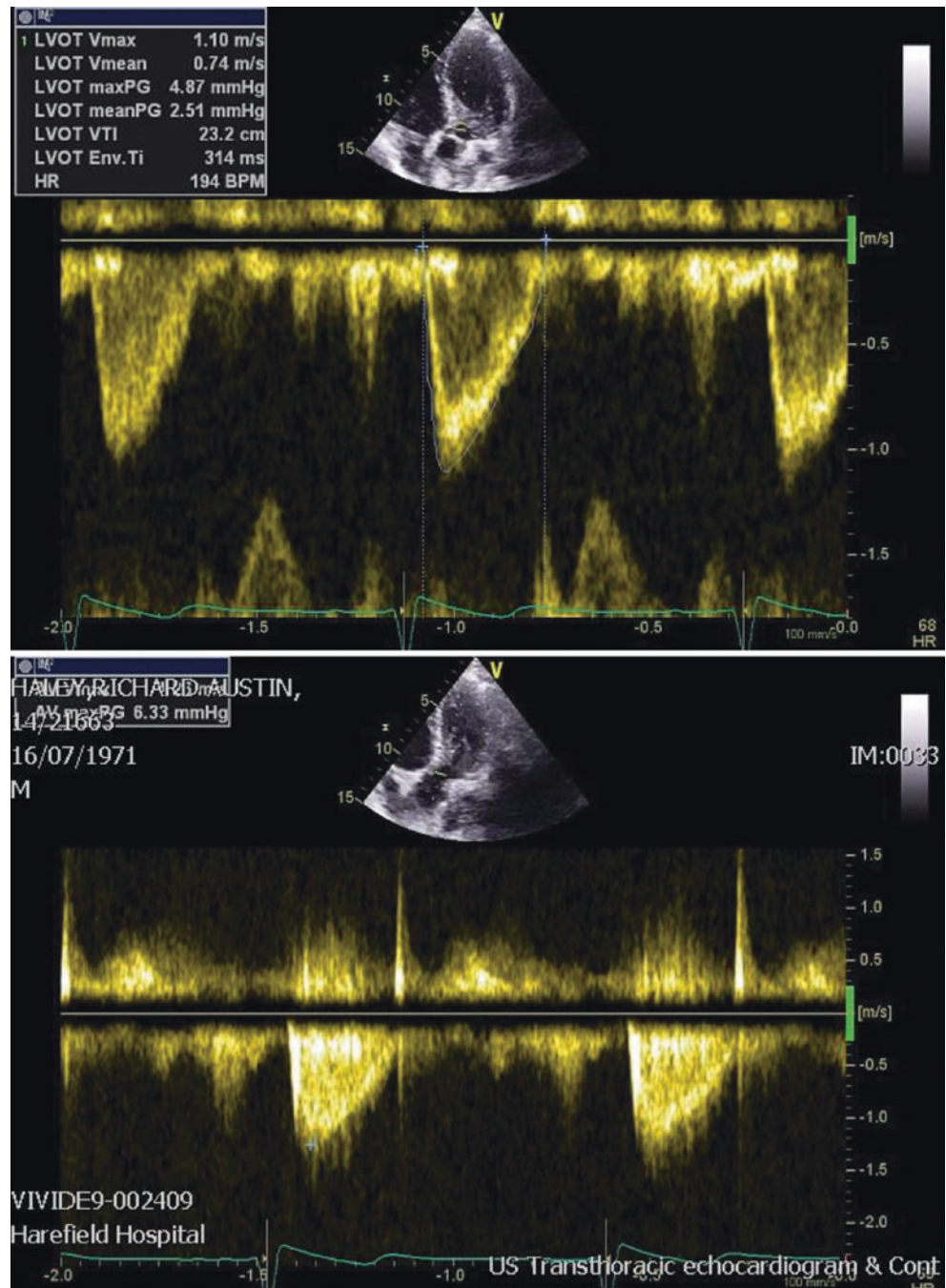
2D two dimensional, CW continuous wave, LVOT left ventricular outflow tract, RVOT right ventricular outflow tract

viewer to easily appreciate abnormal flows such as fistulae, septal defects (Fig. 3.3), regurgitant valve lesions and the turbulence associated with stenotic lesions, attempting to quantify the severity of a lesion from the appearance of the color jet alone is fraught with error and should be avoided.

Tissue Doppler imaging (TDI) uses the Doppler principle to assess the motion of myocardium, most commonly at the lateral and septal mitral annulus and the RV free wall. Abnormal TDI is a good way to confirm early myocardial dysfunction and is also particularly useful when assessing diastolic filling (Fig. 3.4) and when differentiating pericardial constriction from restrictive cardiomyopathy—an E’ at the lateral annulus of ≥ 8 cm/s indicates constriction rather than restriction.

Strain imaging by echocardiography measures the extent of myocardial deformation, i.e. the change in myocyte length during systole. Change in length per unit time is *strain rate*. Either global or regional strain or strain rate can be measured and evidence is growing that strain abnormalities are one of

Fig. 3.2 Top panel shows PW Doppler from a normal left ventricular outflow tract; Bottom panel is CW Doppler across a normal aortic valve. Note that PW traces appear “hollowed out”. This is because most of the signal is coming from one particular depth—in this case approximately 1 cm below the aortic valve



the earliest detectable signs of subclinical contractile dysfunction. The normal value for global mean longitudinal strain is $\geq -19\%$. Marked reductions in global strain are seen in cardiomyopathies, and in particular in infiltrative cardiomyopathies such as amyloidosis (Fig. 3.5).

Three-dimensional (3D) echocardiography is a relatively new development and although initially very exciting, it has taken some time to find its place in the armamentarium. This was probably due to limitations in probe technology in its

early iterations, which limited temporal resolution, especially with color flow Doppler. However, with technological advances, it has become clear that 3D echo has a role to play especially in planning complex surgical procedures such as mitral valve and aortic root repair, in complex congenital heart disease, in the assessment of intracardiac masses including thrombus in the left atrial appendage and in assessing the complications of infective endocarditis [2] (Figs. 3.6 and 3.7).

Fig. 3.3 Colour flow Doppler confirming a large secundum atrial septal defect (arrow) in a 6 year-old boy. Red color indicates blood moving towards the transducer, at the apex of the scan sector

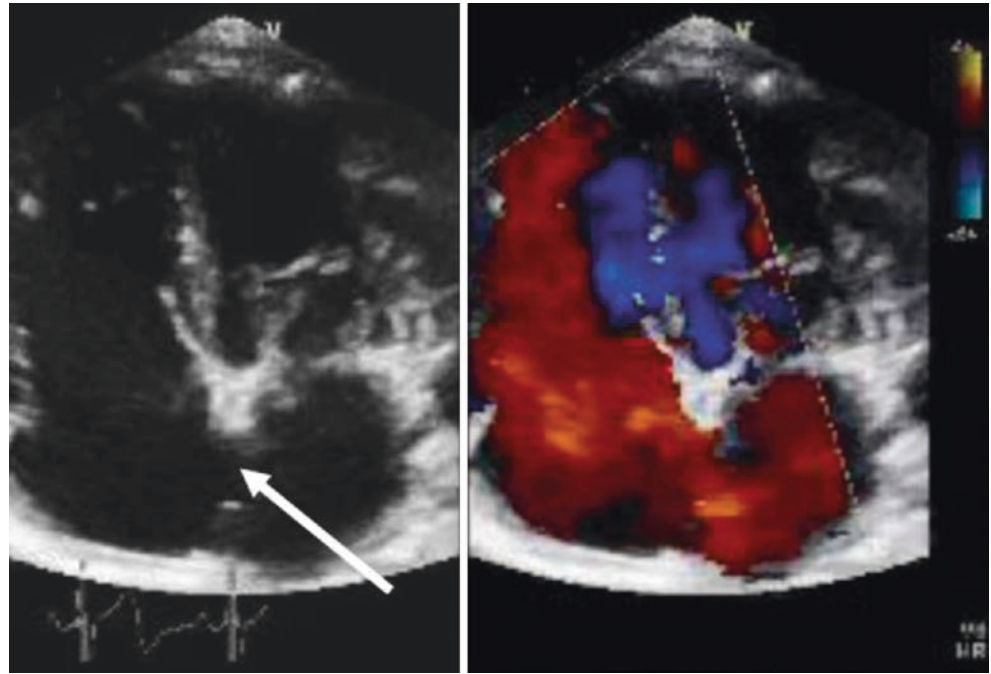
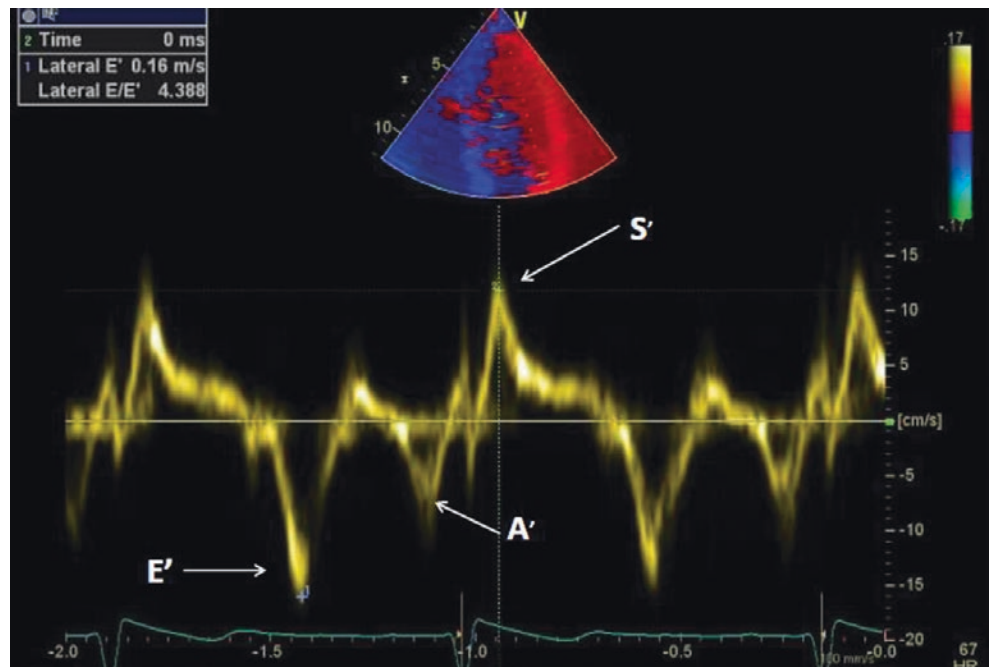


Fig. 3.4 Normal tissue Doppler signals from the lateral mitral annulus. The S' velocity should be >10 cm/s



Assessment of Myocardial Function

Left Ventricular Systolic Function

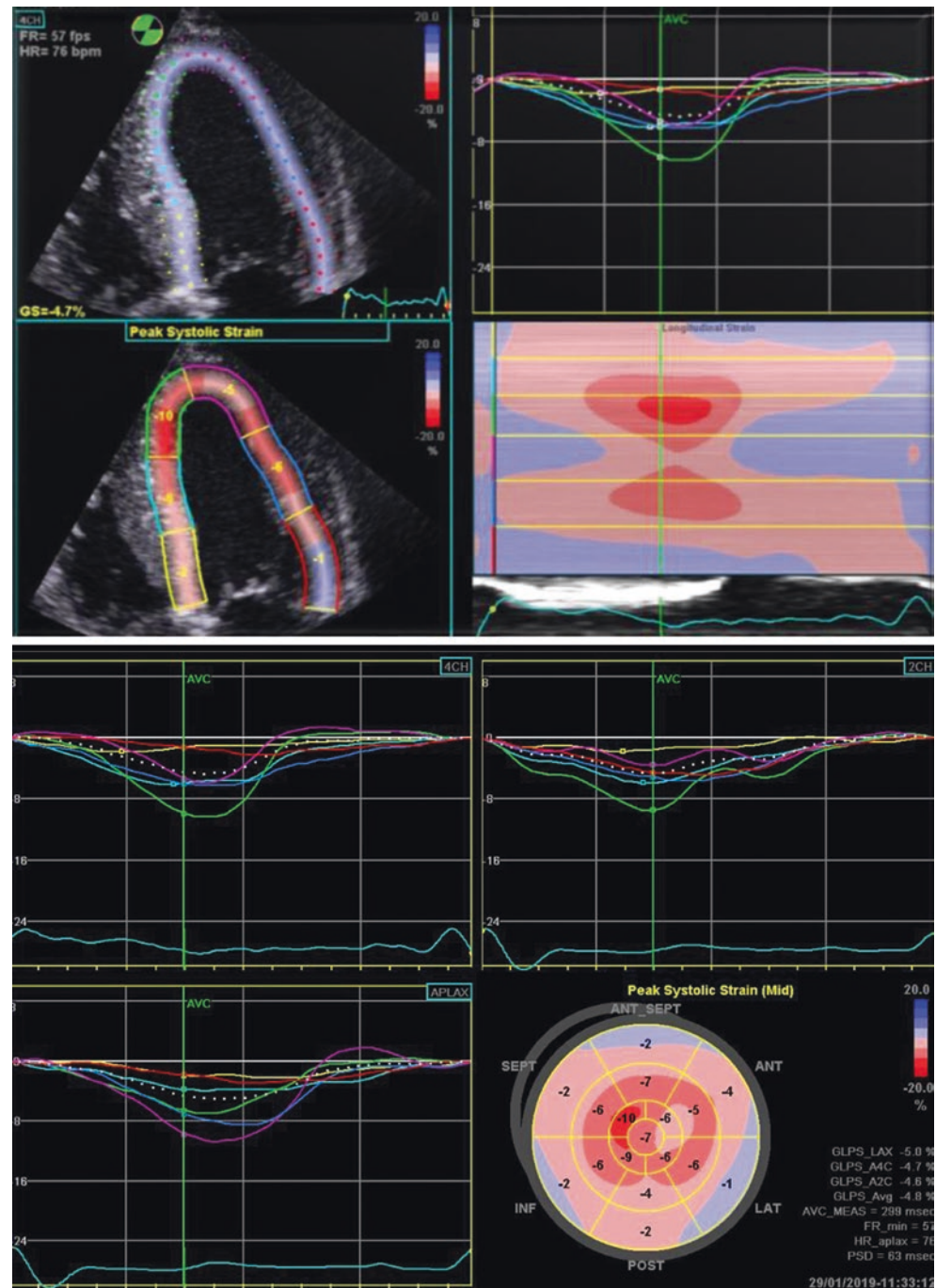
The assessment of myocardial systolic contractile function is done indirectly by echocardiography by assessing three parameters; the change in volumes (2D/3D) or dimensions (2D/M-mode) from diastole to systole, indices of contractility such as the rate of rise of pressure with time (dp/dt) and

Tei index, and strain. None of these is perfect and all are, to a greater or lesser extent, load-dependent.

Changes in Volumes/Dimensions

The most frequently requested and quoted parameter is the *left ventricular ejection fraction* (LVEF) which is the stroke volume expressed as a proportion of the end-diastolic volume. If end-diastolic and end-systolic dimensions are measured by 2D or M-mode then the *fractional*

Fig. 3.5 Strain imaging using 2D speckle-tracking echo—in this patient with amyloidosis, the global mean longitudinal peak strain is severely reduced at -4.8%



shortening (%FS) can be calculated—values for FS are typically half the value of the LVEF in the non-remodeled heart, such as the donor heart after orthotopic transplantation. Fractional shortening measured from M-mode echo is much less relevant in patients with regional contractile abnormalities, as the degree of shortening in one plane may be completely different from that in another. Nowadays, most echo laboratories routinely measure LVEF by either the biplane 2D method (Simpson's biplane method of discs) or by 3D volumetric measurements,

which have been shown to be highly-reproducible. LVEF is highly-dependent on loading conditions and reflects myocardial contractility *only* under the loading conditions at the time at which it is measured. Hence, interpretation of LVEF must be done in the context of those conditions, which may include consideration of the actions of sedative or anesthetic drugs, inotropic agents and valve lesions. For example, in the volume-overloaded heart, such as in severe mitral or aortic regurgitation, LVEF may be elevated, in accordance with the Frank-Starling Law.

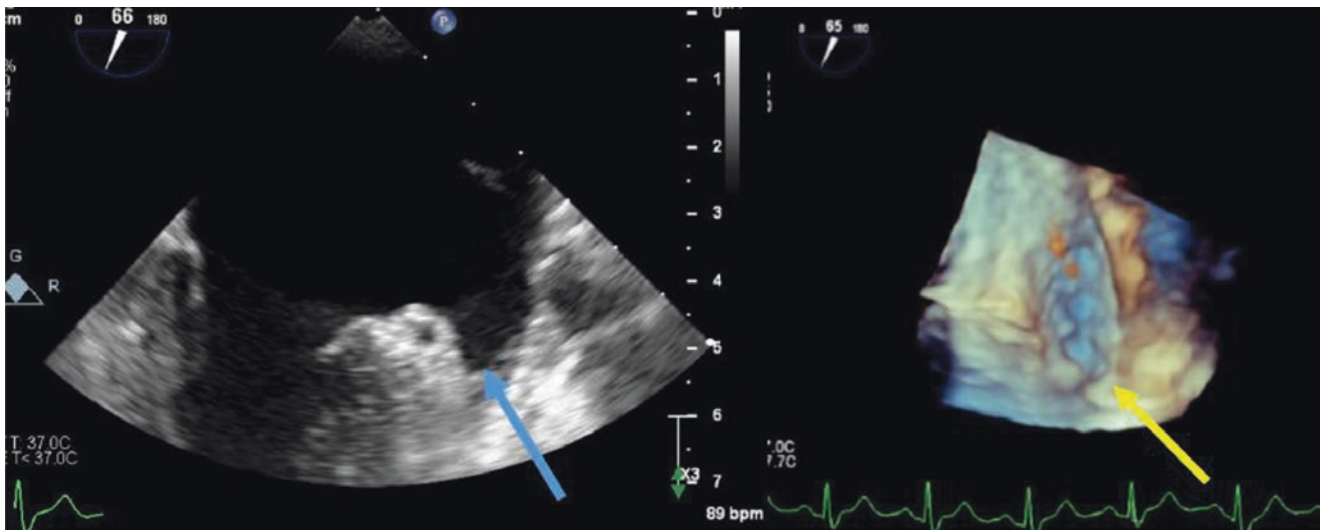


Fig. 3.6 2D transesophageal echocardiography (TEE) of the left atrial appendage showing echoes suspicious for thrombus (yellow arrow) and corresponding 3D TEE confirming that the suspicious “mass” is in fact part of the wall of the appendage (blue arrow)

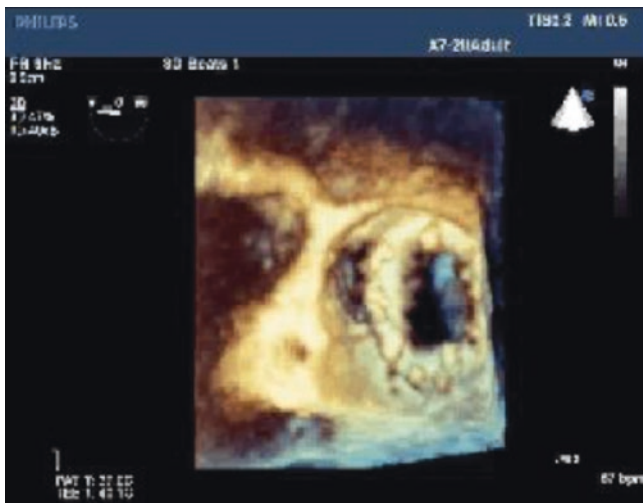


Fig. 3.7 Dehiscent mitral prosthesis seen by 3D transesophageal echocardiography

With the advent of new techniques it has become clear that there are parameters which show abnormalities earlier in the course of LV systolic dysfunction, before there is a change in LVEF or the development of obvious regional abnormalities. Early systolic dysfunction can be detected by assessing abnormalities of long axis function or by assessment of strain using 2D speckle tracking echo. The latter has been shown to be particularly useful in identifying early dysfunction in patients receiving cardiotoxic drugs to treat cancers, and perhaps more relevant to the surgeon, it is becoming clear that even in the presence of an apparently-normal LVEF, subtle abnormalities of strain are predictive of poorer functional outcomes after mitral surgery. It is likely that pre-operative strain measurements will be recognized as valuable prognostic indicators.

Indices of Global Contractility

The rate of development of LV pressure (LV dp/dt) during systole can be assessed from the slope of the mitral regurgitant Doppler waveform (Fig. 3.8). Normal values are >1200 mmHg/s, mild impairment 800–1200 mmHg/s, moderate impairment 600–800 mmHg/s and severe impairment <500 mmHg/s.

The Myocardial Performance Index or *Tei index* is the ratio of the sum of the isovolumic contraction time (ICVT) and the isovolumic relaxation time (IVRT) to the ejection time.

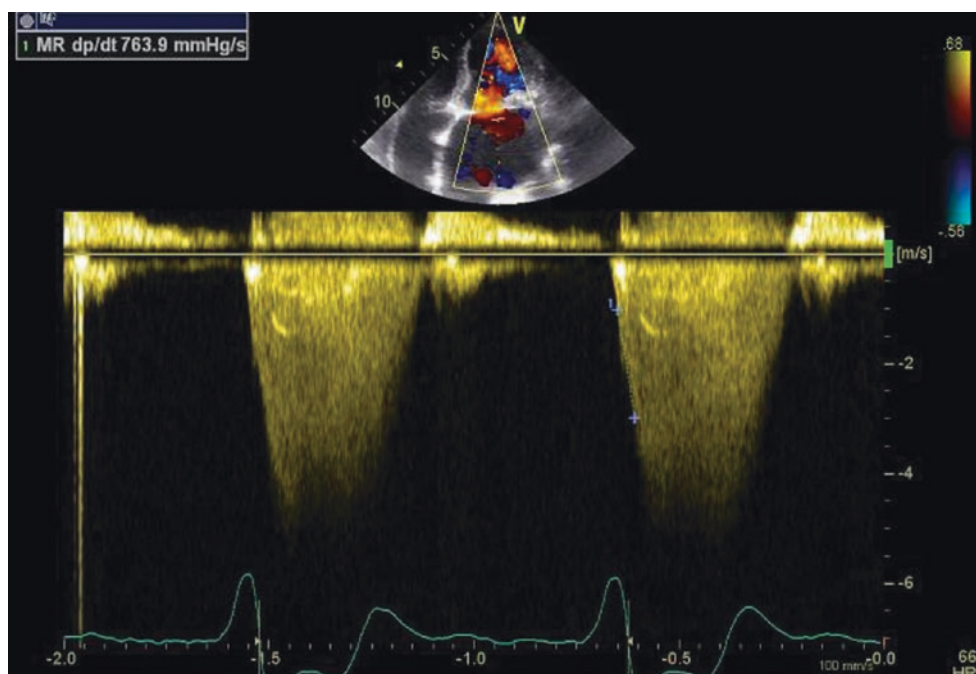
$$\text{Myocardial Performance (Tei) Index} = \text{ICVT} + \text{IVRT} / \text{Ejection fraction}$$

The IVCT is prolonged in systolic dysfunction and the IVRT is prolonged in both systolic and diastolic dysfunction i.e. when there is ventricular dysfunction, the heart spends relatively less time ejecting blood. Tei index is less load-dependent than some parameters, but more time-consuming to calculate and so not performed routinely in most departmental “minimum standards” studies.

Systolic Strain

Global longitudinal strain has now been shown to be a more subtle method of identifying early systolic dysfunction than LVEF. It can also be used prognostically; in a study of heart failure patients every 1% increase in mean GLS was shown to be associated with a 5% decrease in mortality. However, one problem with strain analysis by echocardiography is that currently available proprietary software packages do not give the same results. Hence a patient who is undergoing serial scans for monitoring of function should always have strain analysis done using the same software package.

Fig. 3.8 Measuring the LV dP/dt from the mitral regurgitant signal



Regional Contractile Function

Regional/segmental contractile abnormalities are most commonly seen in ischemic heart disease and represent areas of full or partial thickness myocardial infarction. There are some other more unusual causes of regional abnormalities of contraction but these are less frequently encountered in a surgical setting. The assessment of regional abnormalities has traditionally relied on the experienced eye of the echocardiographer but assessment of endocardial motion alone can be misleading as, in cases where there is a limited segmental infarction, the areas of myocardium adjacent to the infarcted segment may appear to move well but in reality this is due to these regions being tethered to adjacent uninfarcted regions which drag them in. In recent years, software advances have allowed the measurement of segmental systolic strain and strain rate. Demonstration of segmental strain abnormalities gives added confidence to the sonographer when diagnosing a regional abnormality of contraction.

Right Ventricular Systolic Function

The right ventricle (RV) is structurally more complex than the left ventricle (LV) and consequently is more difficult to assess by noninvasive imaging. However, RV function is of great importance, because in any condition affecting the left heart, the addition of impaired RV function increases mortality. As with the LV, all parameters we can currently measure are load dependent. Fractional area change (FAC, normal >31%) and tricuspid annular plane systolic excursion (TAPSE, normal >15 mm) are two easily measured param-

eters, although studies have shown significant variation in the values which predict outcomes in a variety of clinical contexts. As a result, despite the availability of advanced software packages, 3-dimensional volumetric analysis and strain imaging, many surgeons remain most comfortable with the subjective and qualitative opinion of a trusted and experienced echocardiology colleague.

Diastolic Function

The importance of diastolic function in the surgical patient has been increasingly recognized in recent years. It is assessed echocardiographically by measuring the transmitral Doppler E and A waves, and the tissue E' velocity, usually from the lateral mitral annulus. A lateral E/E' value of <10 is normal, values of >15 are abnormal and values of 10–15 represent a “grey area” where there is an increased likelihood of raised filling pressures. The time taken for peak early filling velocity to fall back to zero, the *early deceleration time* is another important parameter. When prolonged, it indicates impaired relaxation and when shortened it may indicate restrictive filling, if the E/A ratio is >2.0 and intraventricular relaxation time is abnormal. If a restrictive filling pattern, also known as a “pseudonormal” pattern, is suspected, a Valsalva manoeuvre should be performed and this should reduce the early filling velocity such that the E/A ratio becomes <1.0. Most patients with abnormal systolic function have some concomitant filling abnormality, and some increase in ventricular stiffness with impairment of relaxation (mild or Grade I diastolic dysfunction) is “normal”

with ageing, but diastolic abnormalities may predominate in patients with LVH such as HCM, aortic stenosis and infiltrative disorders e.g. amyloidosis. In such patients, the impaired ventricular relaxation means that they are highly-dependent on atrial contraction for LV filling, and if they develop atrial fibrillation perioperatively, this can be very difficult to manage, resulting in a downward spiral where increased intravenous filling and inotropes fail to produce an increase in cardiac output. In addition, the surgeon may encounter myocardial protection issues in patients with significant LVH and this may exacerbate the diastolic dysfunction of an already-impaired ventricle. Detailed descriptions of diastolic filling patterns indicative of different degrees of dysfunction can be found in any standard echo textbook. However, from the surgeon's point of view, it is more useful simply to know if diastolic function is normal, mild, moderately or severely impaired as this is likely to have an impact on the patient's postoperative/intensive therapy unit (ITU) course.

Assessment of Valve Pathology

Aortic Stenosis

The appearance of the valve is considered first—the morphology and motion of the leaflets, any degenerative changes and the degree of calcification, which is categorized qualitatively as mild, moderate or severe. Color flow Doppler is used to assess turbulence through the valve and then pulse and continuous wave Doppler is used to measure the velocity of blood flow in the left ventricular outflow tract (LVOT) and through the valve respectively. The pressure drop or “gradient” across a narrowed valve is calculated using a simplified Bernoulli equation, where pressure drop (gradient) $\Delta P = 4V^2$ (V is the maximum velocity of blood flow through the valve) (Table 3.2). In cases where the LVEF and flow rate are normal, a velocity of 4 m/s across the aortic valve (gradient of 64 mmHg) is indicative of severe aortic stenosis (AS). The shape of the CW Doppler waveform is also a clue to severity—as AS advances from “just-about-severe” to “critical” the shape of the trace changes from being asymmetrical with a faster upstroke to becoming symmetrical or “dagger-shaped” (Fig. 3.9) However, in many cases, the LVEF and flow rate are reduced and in these cases it can be much more difficult to appreciate the degree of valve stenosis. Other useful measures are the effective orifice area (EOA) and the dimensionless velocity index (Table 3.3). Calculation of EOA is done using the continuity equation, shown below, where CSA is the cross-sectional area of the LVOT, VTI_1 is the subaortic velocity-time integral and VTI_2 is the transaortic velocity-time integral.

Table 3.2 Examples of surgically-relevant information obtained by echocardiography in different patient groups^a

Patient group	Information obtained by echocardiography	Relevance to surgeon
Ischemic heart disease for revascularization	Global and regional left ventricular function, LVEF	Impaired ventricular function is a significant risk factor for decreased survival; surgeon may choose not to revascularize fully-infarcted areas (especially if this would be technically-difficult or there is the need to reduce bypass time)
Mitral regurgitation	Left and right ventricular function; severity and mechanism of regurgitation, tricuspid valve function	Reduced left and right ventricular function may result in difficult wean from bypass; RV failure may prolong intensive care; tricuspid annuloplasty may be performed if tricuspid annulus is dilated >40 mm
Aortic stenosis	Aortic valve and root dimensions, myocardial thickness, diastolic function	Choice between prostheses; valve or root replacement; moderate-severe left ventricular hypertrophy may cause myocardial protection issues; diastolic dysfunction may prolong ITU stay if filling is very impaired especially if there is perioperative atrial dysrhythmia
Aortic regurgitation	Aortic root dimensions, valve morphology, ventricular function	Choice of operative strategy—valve replacement or repair, root replacement, valve-sparing root surgery?
Endocarditis	Evidence of complications e.g. fistulae and abscess formation	Informs operative planning regarding likely length and complexity of surgery

ITU intensive therapy unit, LVEF left ventricular ejection fraction, RV right ventricular

^aThis is NOT comprehensive

$$\text{Flow-corrected EOA} = \text{Subaortic CSA} \times VTI_1 / VTI_2$$

The calculation uses the square of the radius of the LVOT, which relies on accurate measurement of the LVOT diameter. Any error in this measurement is compounded by the squaring operation and hence is a significant source of error in the calculation of EOA. The dimensionless velocity index is the ratio of maximum flow velocity in the LVOT to maximum flow velocity through the stenotic valve. It eliminates error due to inaccurate measurement of the LVOT diameter.

Fig. 3.9 The symmetrical “dagger-shaped” CW Doppler trace seen in very severe aortic stenosis

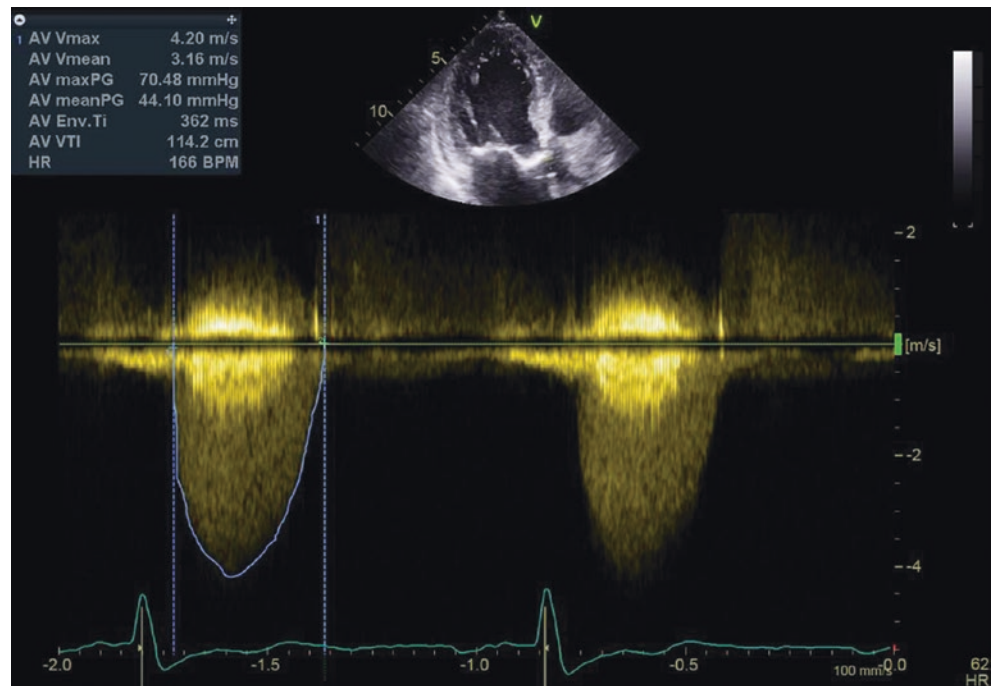


Table 3.3 Criteria for assessing severity of aortic stenosis

Criterion	Mild	Moderate	Severe
Vmax (m/s)	2.5–3.0	3.0–4.0	>4.0
Peak gradient (mmHg)	<40	40–64	>64
Mean gradient (mmHg)	<25	25–40	>40
Effective orifice area (cm ²)	>1.2	0.8–1.2	<0.8
Dimensionless velocity index	>0.5	0.25–0.5	<0.25

The 2017 ESC Guidelines on the management of valve disease [3] recognizes four different categories of aortic stenosis, based on flow and LVEF (Table 3.4).

Aortic Regurgitation

The etiology of aortic regurgitation generally falls into one of two broad categories: valve abnormalities (congenital, infective, rheumatic, degenerative and other rarer causes) and root dilatation. The latter is commonly associated with longstanding hypertension, as well as being a feature of Marfan’s, Loays-Dietz and Ehlers-Danlos syndromes along with other collagen vascular disorders not yet genetically-characterized. Aortic valve and root morphology is visually assessed and aortic dimensions are measured at standard levels: the LVOT, the “annulus”, across the sinuses of Valsalva, the sino-tubular junction and the ascending aorta (Fig. 3.10). The vena contracta of the color jet is measured and the width of the regurgitant jet is also expressed as a percentage of the LVOT diameter 5–10 mm below the valve (Fig. 3.11). As with mitral regurgitation, the PISA method

may be used to calculate EROA and regurgitant volume. The most commonly-quoted parameter is the pressure half-time, measured from the CW Doppler trace. This can be misleading in advanced disease, because the pressure half-time is shortened in the presence of raised end-diastolic pressure. The density of the regurgitant signal is also compared visually to the density of the forward flow trace. LV volumes and LVEF are also important because a hyperdynamic ventricle suggests severe regurgitation and a dilated ventricle usually means the regurgitation is chronic. Perhaps the most sensitive parameter is the demonstration of pandiastolic flow reversal in the descending limb of the aortic arch by color flow or PW Doppler. Parameters used to assess the degree of aortic regurgitation are shown in Table 3.5.

Mitral Stenosis

This is seen less frequently in the West due to the decline in prevalence of rheumatic heart disease. However, worldwide it continues to be the commonest cause of mitral stenosis (MS). The “hockey stick” appearance of the anterior mitral leaflet is diagnostic (Fig. 3.12). Echocardiography is excellent for demonstrating calcium in the leaflets and subvalvar apparatus and the degree of stenosis may be assessed using Doppler parameters such as pressure half-time (mitral valve area (cm²) = 220/pressure half-time (ms)) and planimetry. (Severe MS <1 cm², moderate 1.0–1.5 cm², mild >1.5 cm²) When considering whether balloon valvuloplasty may be

Table 3.4 Types of aortic stenosis recognized in the 2017 ESC Guidelines for the management of valve disease

Type of aortic stenosis	Mean gradient	Area	Flow	LVEF	Notes
High PG	>40 mmHg	<1 cm ²	Normal/reduced	Any	For surgical intervention, bearing in mind that lower LVEF increases risk
Low-flow, low PG, low LVEF	<40 mmHg	<1cm ²	Reduced (SVi < 35 ml/m ²)	<50%	Role for DSE
Low flow, low PG, Normal LVEF	<40 mmHg	<1cm ²	Reduced	≥50%	Older, female, LVH, BP MSCT calcium score
Normal flow, low gradient, normal LVEF	<40 mmHg	<1cm ²	Normal (SVi >35 ml/m ²)	≥50%	Moderate AS (in general..)

AS aortic stenosis, BP blood pressure, DSE dobutamine stress echo, LVEF left ventricular ejection fraction, LVH left ventricular hypertrophy, MSCT multislice computed tomography, PG peak gradient, SVi stroke volume index

Fig. 3.10 The normal aortic root seen in a TEE lower esophageal view at approximately 120° showing aortic measurements made at various standard levels

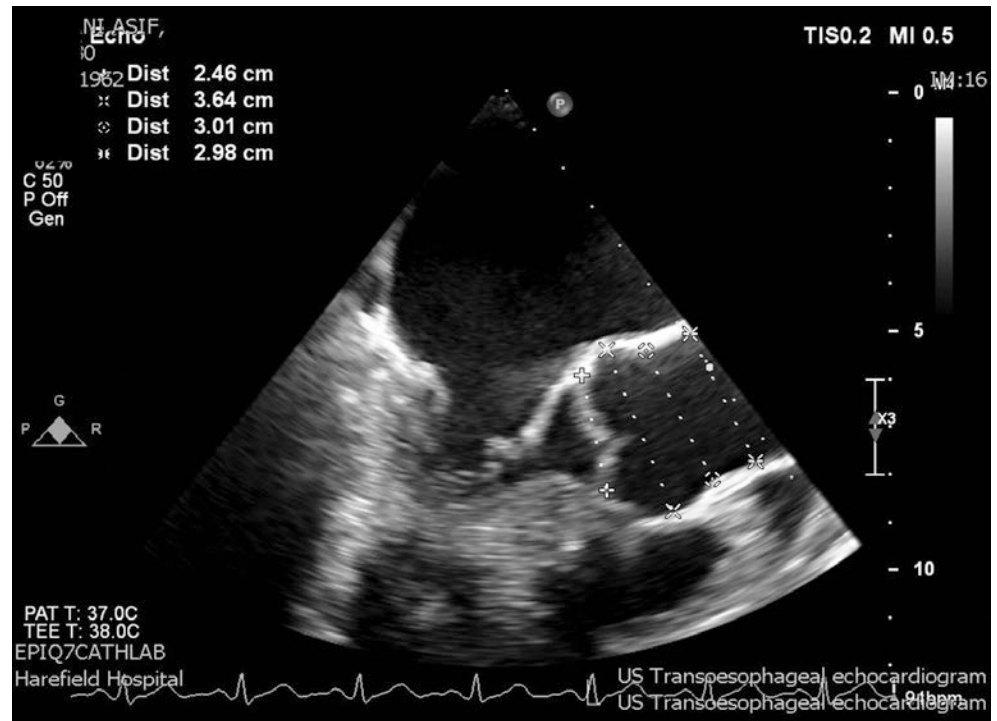


Fig. 3.11 Jet width in the left ventricular outflow tract in aortic regurgitation. Panel a—mild, Panel b—severe

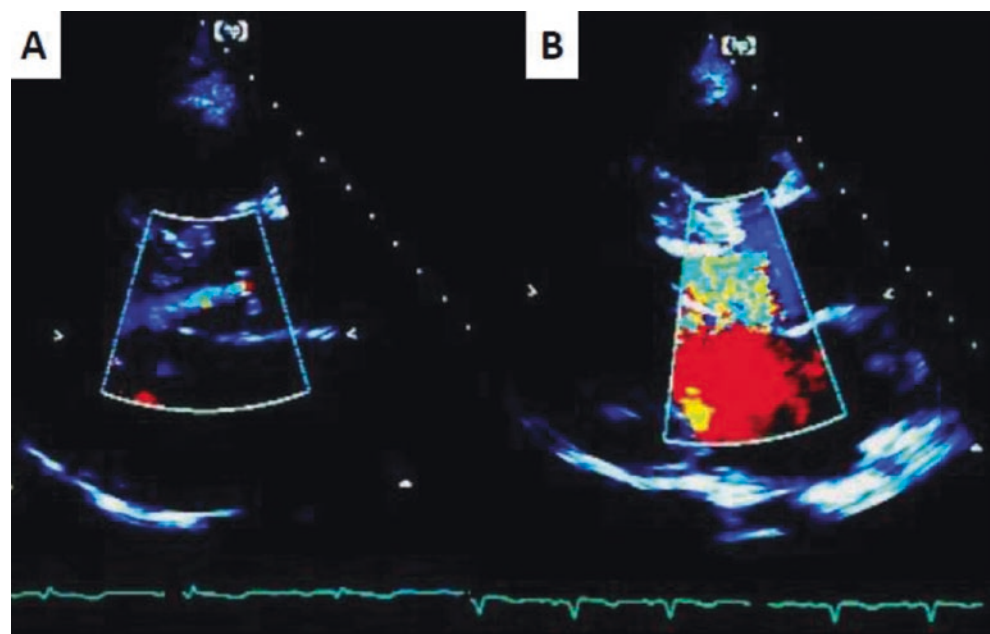


Table 3.5 Criteria for assessing severity of aortic regurgitation

Criterion	Mild	Moderate	Severe
Jet width as % of LVOT width	<30	31–60	>60
Pressure half-time (ms)	>650	250–650 BUT this is a very grey area, with mild and severe AR sometimes falling into this category by PHT measurement, which can be affected by a number of other factors such as LVEDP	<250
Density of CW Doppler trace	Faint or incomplete	Complete but not as dense as forward flow	As dense as forward flow Doppler trace
Vena contracta (mm)	<3	3–6	>6
Flow reversal in the descending limb of the arch	None/early “flash” due to aortic recoil	Present but not pandiastolic	Pandiastolic/long diastolic tail

AR aortic regurgitation, LVEDP left ventricular end-diastolic pressure, LVOT left ventricular outflow tract, PHT pulmonary hypertension

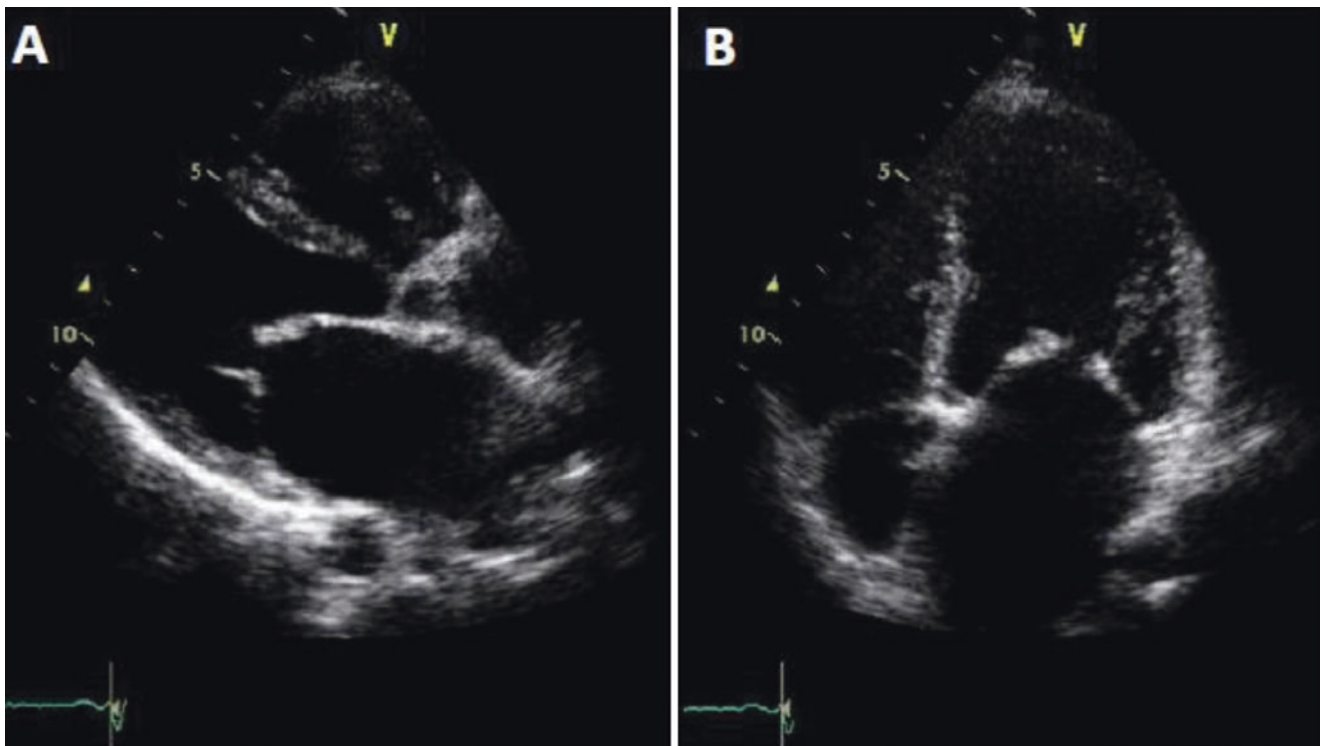


Fig. 3.12 Parasternal long axis (a) and 4-chamber (b) views showing a rheumatic mitral valve—note the typical “hockey stick” appearance of the anterior leaflet

more appropriate for the patient than surgery, the Wilkins Score may be used to assess the likelihood of a favorable outcome. The score is based on echo appearances and rates the valve for leaflet mobility, leaflet thickening, calcification and subvalvar involvement. The maximum score for each category is 4 and the minimum is one, hence the scores range from 4 to 16. A score of 8 or below is predictive of a favorable outcome with balloon valvuloplasty. Some measurements may be less reliable in the presence of other valve lesions, and in many cases, a detailed examination by transesophageal echocardiography is helpful to clarify the situation.

Mitral Regurgitation

Echocardiography is key to distinguishing between primary degenerative mitral valve disease and secondary mitral regurgitation (MR) due to abnormalities of LV geometry and function (Fig. 3.13). A systematic approach to the assessment and grading of MR involves assessment of the morphology of the valve, the annulus, leaflets, subvalvar apparatus and papillary muscles. Color flow Doppler is used to demonstrate the regurgitant jet, although relying on this alone for the estimation of severity of MR is inadvisable. The most distinguishing parameter for severity of MR in the awake patient is the

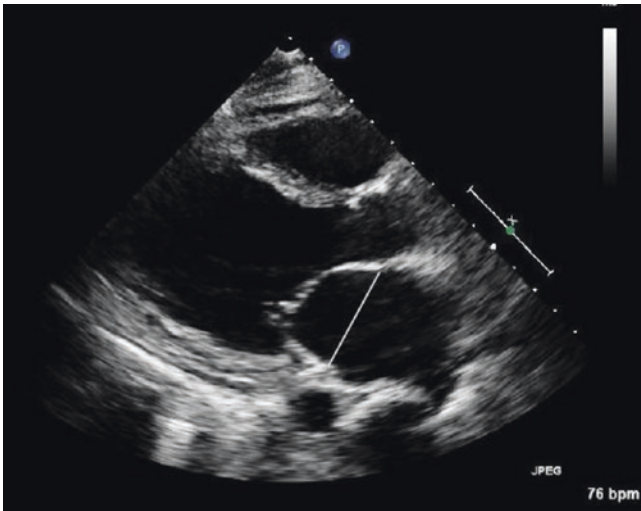


Fig. 3.13 Mitral leaflets tethered in to the left ventricle due to adverse ventricular geometry and increased interpapillary muscle distance. The annular plane is marked by the white line

transmitral PW Doppler trace. In severe MR, the early filling (E wave) should be ≥ 1 m/s. An assessment of pulmonary pressure should be made from the tricuspid regurgitant signal, if present. The PISA equation can be used to calculate effective regurgitant orifice area and regurgitant volume. It must be remembered that for the same calculated MR regurgitant volume, the prognosis for degenerative MR is better than that for ischemic functional MR. This has led many experts to suggest that “moderate MR” in ischemic patients is “in reality severe MR”. However, the author is of the opinion that the MR volume is exactly what it is measured as—it is the prognosis that differs depending on the etiology. The box below is a list of suggested questions that the surgeon should ask him/herself when reviewing echo images during heart team discussions of mitral regurgitation cases.

- What is the jet width?
- How dense is the Doppler trace?
- What are the EROA and regurgitant volume by PISA calculation?
- How big is the left atrium?
- Is the filling pattern consistent with severe MR?
 - Short filling time?
 - High-velocity E wave?
- Is there presystolic MR?
- Is there systolic blunting/reversal of the pulmonary venous flow signal?
- What is the mechanism?

Transthoracic echocardiography is more than adequate to assess the severity of native mitral valve regurgitation, but in patients who are likely to require surgical or percutaneous

mitral intervention, the exact mechanisms of the MR are best shown by a detailed transesophageal echo, including 3D imaging or reconstruction.

Tricuspid Valve Assessment

As with other valves, the first question is whether the valve is morphologically normal. Abnormalities of the leaflets should be noted, along with assessment of the annulus and RV. Causes of tricuspid regurgitation (TR), as with MR fall in to two broad categories—primary valve disease and secondary ventricular/functional etiology. Echo criteria for grading the severity of TR include the density and shape of the CW Doppler trace, the vena contracta width and the presence of hepatic vein systolic flow reversal or blunting. Pulmonary artery systolic pressure (PASP) may be estimated by measuring the pressure drop across the tricuspid valve from the TR CW Doppler signal and adding this to the right atrial (RA) pressure estimated from the inferior vena cava (IVC) dimension and inspiratory reactivity. However, in cases of severe chronic TR where the pressures in the RA and RV have virtually equalized, the TR signal is no longer a reliable method of estimating PASP.

Pulmonary Valve Assessment

The normal pulmonary valve is mildly regurgitant. The regurgitant signal may be used to estimate pulmonary artery end-diastolic pressure, using the end-diastolic velocity of the regurgitant signal, whether normal (physiological) or pathological. Pulmonary valvar abnormalities are seen predominantly in patients with congenital heart disease, although there are a few conditions which are known to affect predominantly right-sided valves, including carcinoid syndrome and device-associated infective endocarditis.

Infective Endocarditis

Echocardiography has long been the first-line imaging test performed on patients with suspected endocarditis. Despite this, it was only relatively recently that the criteria for diagnosing endocarditis were modified to include echo evidence of infection as one of the major criteria. Any of the four native valves in the heart can be infected, but the initial source of infection is elsewhere in the body—the heart is very rarely the primary source [2]. In the mid to late twentieth century, the commonest suspected source of bacteremia was the mouth, with oral streptococci being the usual culprits. In some cases, a temporal relationship to dental work can be demonstrated. Skin organisms such as staphylococci and in particular the very invasive *S. aureus* were the other commonly-seen infective organisms—often in association

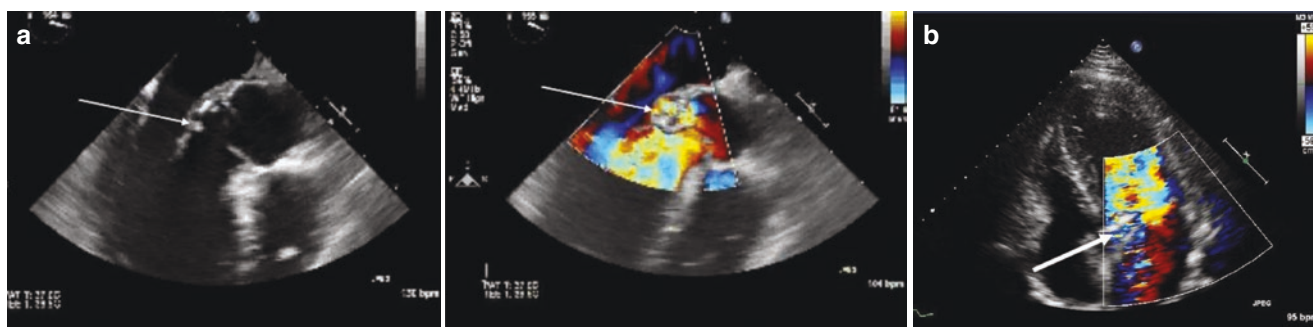


Fig. 3.14 (a) Aortic root abscess (arrow) seen by TEE with color flow Doppler and severe aortic regurgitation in a patient with infective endocarditis. (b) In this patient with aortic endocarditis, a fistula (arrow) has formed between the aortic root and the left ventricle

with intravenous drug use, and primarily affecting the venous or right side of the heart. However, many other organisms, both bacterial and fungal, are known to be causally implicated in endocarditis. Recently, there has been a significant rise in infections in patients who have implantable cardiac devices. This so-called “device-associated endocarditis” is commonly caused by skin organisms. Prosthetic material in the heart, whether it be artificial valves, Dacron patches and conduits or pacing leads may all present focuses for infection. Organisms in the bloodstream become attached to the prosthetic material and form infected clumps composed of organisms, fibrin, and blood cells, termed a *vegetation*. Once prosthetic material is involved, it is virtually impossible to clear the infection and effect a cure without removing the infected material. Despite advances in virtually all fields of medicine and in particular in the field of infectious diseases, the mortality from infective endocarditis has remained depressingly constant at 25–40%, with infected prosthetic material, such as heart valves, carrying the highest mortality and morbidity rates. The reasons for this include delay in diagnosis and the increased age and hence frailty of many patients, especially in the device-associated infection group.

Echo Findings in Endocarditis

Typically, echocardiography demonstrates vegetations as mobile intracardiac masses, often associated with any prosthetic material or artificial valve. The size, shape and mobility of vegetations varies greatly depending on a number of factors including the type of organism involved, the exact site of the lesion and the amount of free space in which the vegetation can move. Other findings reflect the damage caused to endocardial structures by the invasive infecting organism—these findings include fistulae between chambers, abscesses of the aortic root and mitral annulus/leaflets, destruction of tissue e.g., valve leaflets, and dehiscence of prosthetic valves or graft material. The consequences of such destruction often produces new regurgitant valve lesions, paravalvar leaks, abscesses and shunting between chambers

and/or great vessels—demonstrable by abnormal color flow Doppler findings (Fig. 3.14a, b).

Transesophageal echocardiography (TEE) is significantly more sensitive than transthoracic echo for visualizing vegetations (approximately 90% vs. 60% respectively), especially in the presence of prosthetic material which causes echo artefacts. Real time 3D TEE has proven to be very useful in this regard, and is also useful for confirming paravalvar leaks.

It must be noted that, despite advances in echo, it is entirely possible for echocardiographic appearances to be normal in the presence of intracardiac infection, hence, the diagnosis of infective endocarditis rightly remains a clinical one.

Pericardial Disease

Echocardiography is the technique of choice to confirm the presence of pericardial effusion. In the cardiac surgical patient this is most commonly a request made during the early post-operative course, but there are some later-presenting cases at 3–6 weeks post-operatively due to Dressler’s syndrome. Preoperative assessment of effusion is also made in the oncology patient, or patients with other pericardial diseases. Echo plays two roles: firstly, confirming the presence of pericardial fluid and differentiating it from pleural fluid, and secondly assessing any haemodynamic effects of the effusion. The accumulation of pericardial fluid can cause tamponade, a clinical syndrome in which elevated intrapericardial pressure restricts filling of the heart, hence reducing cardiac output. It cannot be sufficiently emphasized that tamponade is a clinical diagnosis, based on the findings of Beck’s triad: true or relative hypotension, distended neck veins and muffled or absent heart sounds, often with an associated tachycardia. Unfortunately for those relying on clinical examination in the postoperative patient, heart sounds may be less distinct due to inflammation and tissue edema, bruising or iv catheters may make it difficult to appreciate the neck veins, the patient may be

paced and there are other reasons for hypotension. Nevertheless, tamponade is relatively unlikely in a completely well, asymptomatic postoperative patient with stable blood pressure and heart rate.

The typical findings are of an echo-free space around the heart (Fig. 3.15). The first priority is to distinguish pericardial from pleural fluid. If the echo-free space extends behind the aorta, then this is a pleural collection. The size of the space is directly correlated with the fluid volume. In cases where this is large, the ventricle may appear to be moving within the

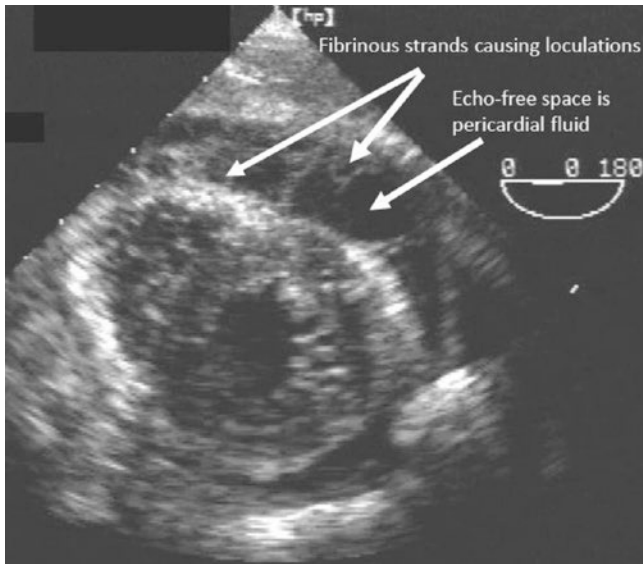


Fig. 3.15 Loculated pericardial effusion seen by TEE in transgastric view

fluid—the so-called “swinging heart”. In the postoperative patient the fluid may be circumferential or loculated, and associated with the right or left sides of the heart or both. The sonographer will assess the volume of fluid, and then any hemodynamic effects by assessing cardiac inflow and outflow Doppler across the mitral, tricuspid and aortic valves during respiration. Typically, there should be <20% variation in the amplitude of the inflow Doppler during respiration. However, in the post-operative patient, this may be confounded by the patient’s filling status and by positive pressure ventilation, which splints the IVC. The most significant finding in the awake, spontaneously-breathing patient is of an engorged IVC which does not reduce in size when the patient performs a short, sharp intake of breath, the “sniff test”.

Pericardial constriction can be challenging to diagnose by echocardiography, but as mentioned above, tissue Doppler imaging can distinguish between constriction and restriction in many cases.

Masses

The most commonly encountered masses in the heart are thrombi due to low flow or thrombophilia traits. Thrombi are particularly seen in the left atrial appendage of patients in atrial fibrillation and lining the wall of akinetic aneurysmal infarcted areas of the left ventricle. Contrast may be used to confirm the presence of thrombus. Tumors of the heart are much rarer but may be either primary, such as myxomata and fibroelastomata (Fig. 3.16), or secondary such as renal or breast metastasis and malignant melanoma.

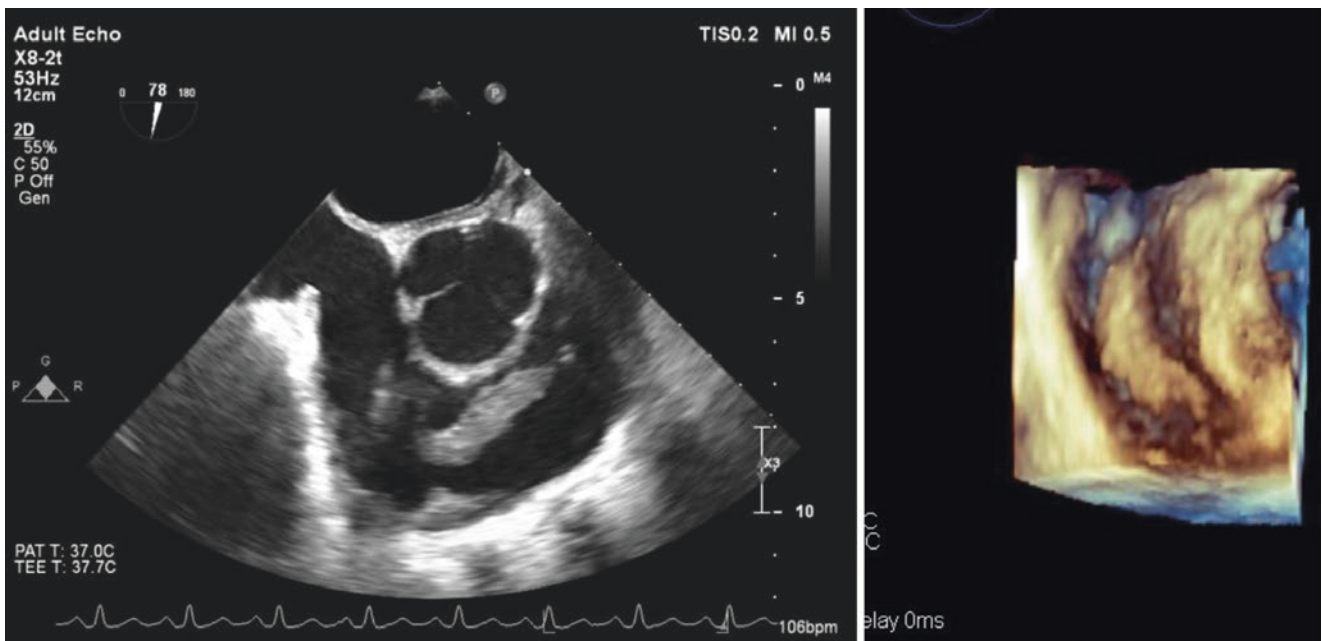


Fig. 3.16 2D and 3D echo of a mass in the right ventricle in a patient who presented with pulmonary embolism—this was a myxoma